Effective Spin Foams & the Flatness Problem

International Loop Quantum Gravity Seminar
September 29th, 2020

Hal M. Haggard
Bard College

Based on joint work [arXiv:2004.07013]

with Seth K. Asante and Bianca Dittrich

In Regge Calculus we approximate spacetime by a triangulation of flat pieces glued together to give curvature.

Discrete Areas & Geometrical Path Integrals

This cuts the degrees of freedom of gravity down to a finite number and eases study.

It is also essential for doing numerics.

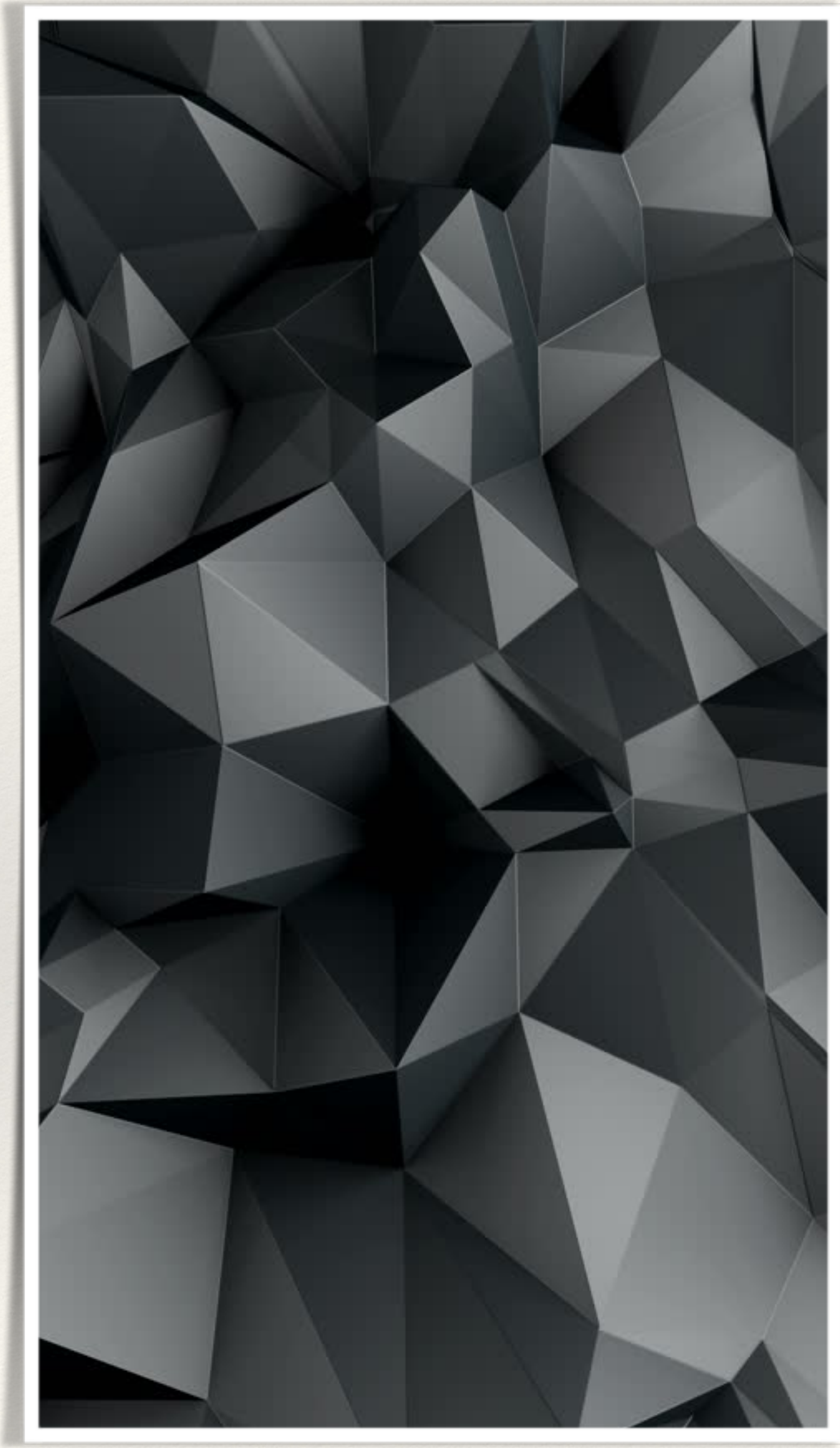

A dimensional ladder helps to illustrate some salient aspects of Regge Calculus

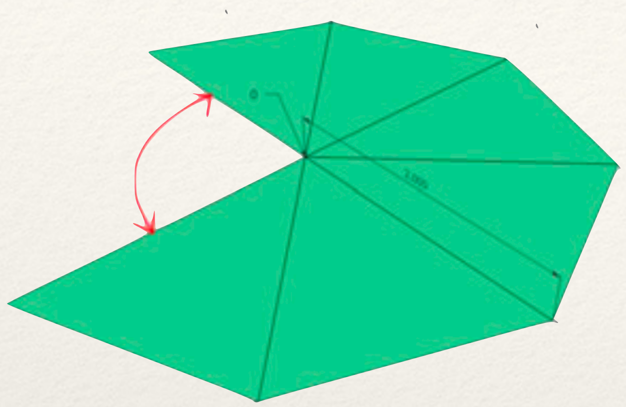

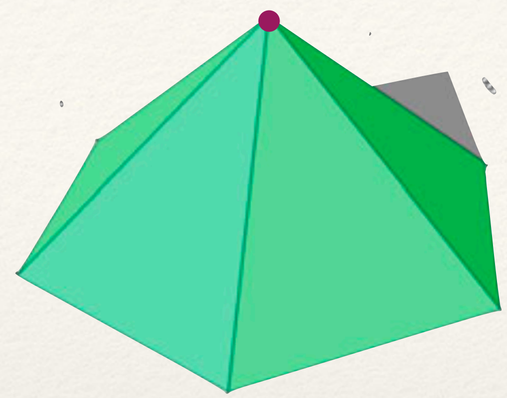

2D

In 2D it is clear how curvature becomes concentrated on the $(d - 2)$-dimensional 'bones'.

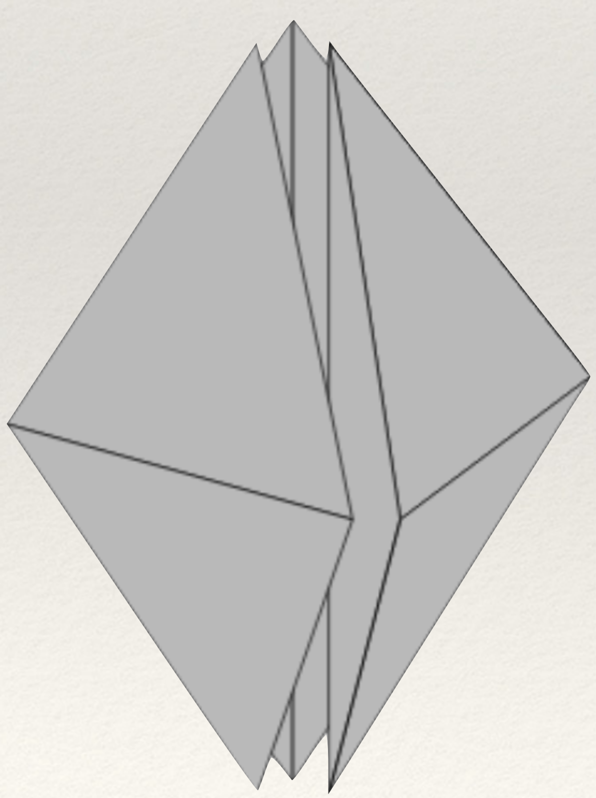

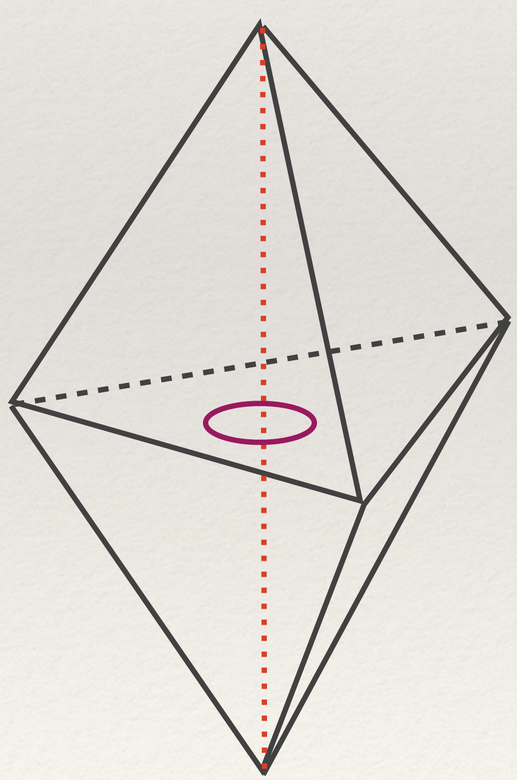

3D

In 3D we see an intriguing alignment between the *metrical* and *symplectic* aspects: the bones are 1D edges, whose lengths give the metric;

meanwhile the conjugate curvature angle is compact and leads to quantization of lengths

A dimensional ladder helps to illustrate some salient aspects of Regge Calculus and 4D is particularly rich

In 4D the bones are 2D triangles *t*.

One is forced to choose between: the apparent metrical length variables *l*, with a complicated conjugate variable

or

The curvature angle around the bone, which is conjugate to the area of the triangle *t*. Again as the curvature angle is compact, the areas are quantized.

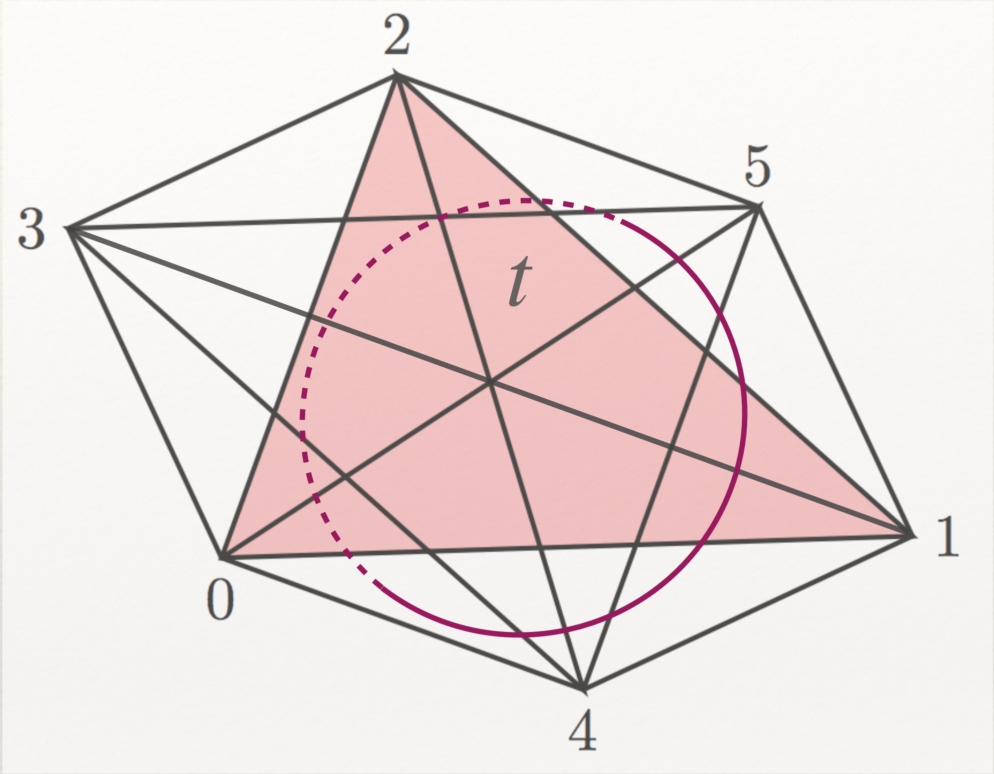

The 2nd choice is harmonious with LQG.

Our motivations for investigating a new spin foam model

▲ Our aim is to build the simplest possible quantum gravity amplitudes that incorporate the (LQG) discrete area spectrum:

$$a(j) = \gamma \ell_P^2 \sqrt{j(j+1)} \sim \gamma \ell_P^2 (j + 1/2), \quad \text{with} \;\; \ell_P = \sqrt{8\pi\hbar G/c^3}.$$

γ is the Barbero-Immirzi parameter

▲ To this end we cast the action in terms of area variables

▲ The unconstrained action has only flat classical solutions, which leads us to impose constraints on the theory

▲ However, our choice of discrete area spectrum disallows strong imposition of these constraints; we investigate the strongest possible (weak) imposition consistent with the area spectrum

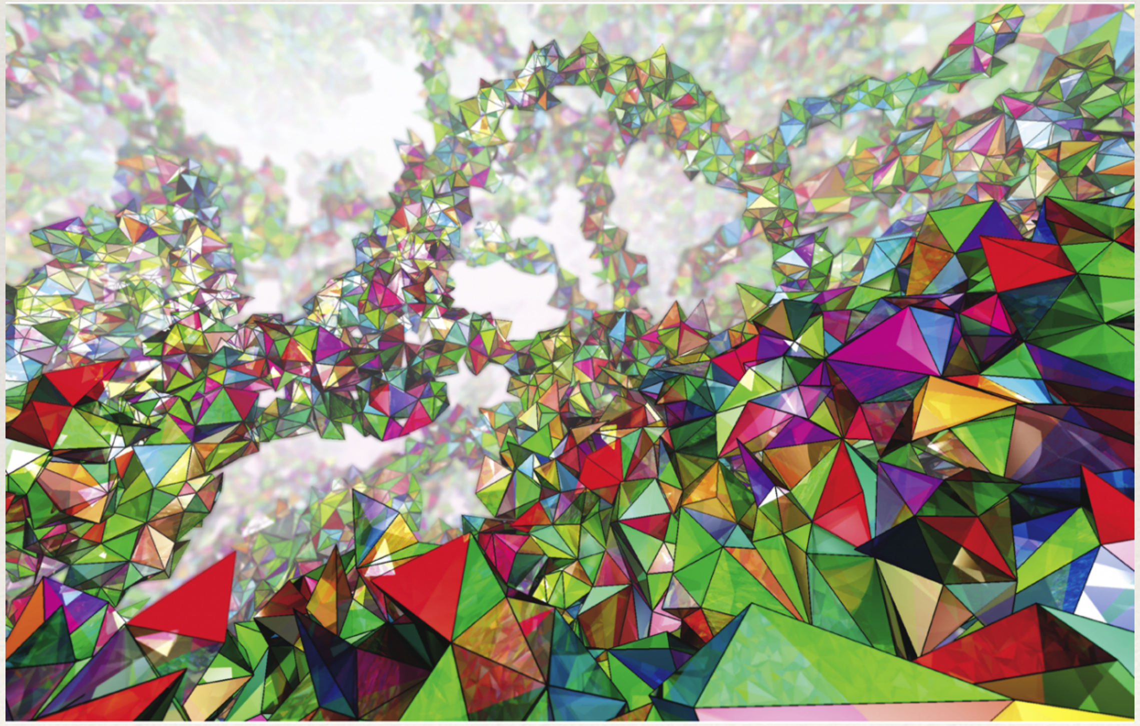

▲ What results is a remarkably accessible and computable model

Defining the Model: an *Outline* of the talk

To understand the ingredients of the model we will:

1. See how area variables lead to flat classical solutions in the unconstrained theory.
2. Study constraints that can be imposed on a classical theory cast in these variables and discover why they can only be imposed weakly in the quantum theory.
3. Define the (Euclidean signature) model. This model has the structure of a standard spin foam with weights defined on triangles and 4-simplices with the addition of a particular constraint on the tetrahedra along which two 4-simplices are glued.

With the model in hand, I will report on numerical investigations we have performed on two different triangulations. In both cases we find, in a particular limit, good agreement with the classical solutions imposed by the boundary data.

In standard Regge Calculus we treat the lengths of edges as vars, while in Area Regge Calculus it's the areas of triangles

The Regge Action for a 4D triangulation Δ is

$$S_{\text{Regge}} = \sum_t A_t \epsilon_t \,,$$

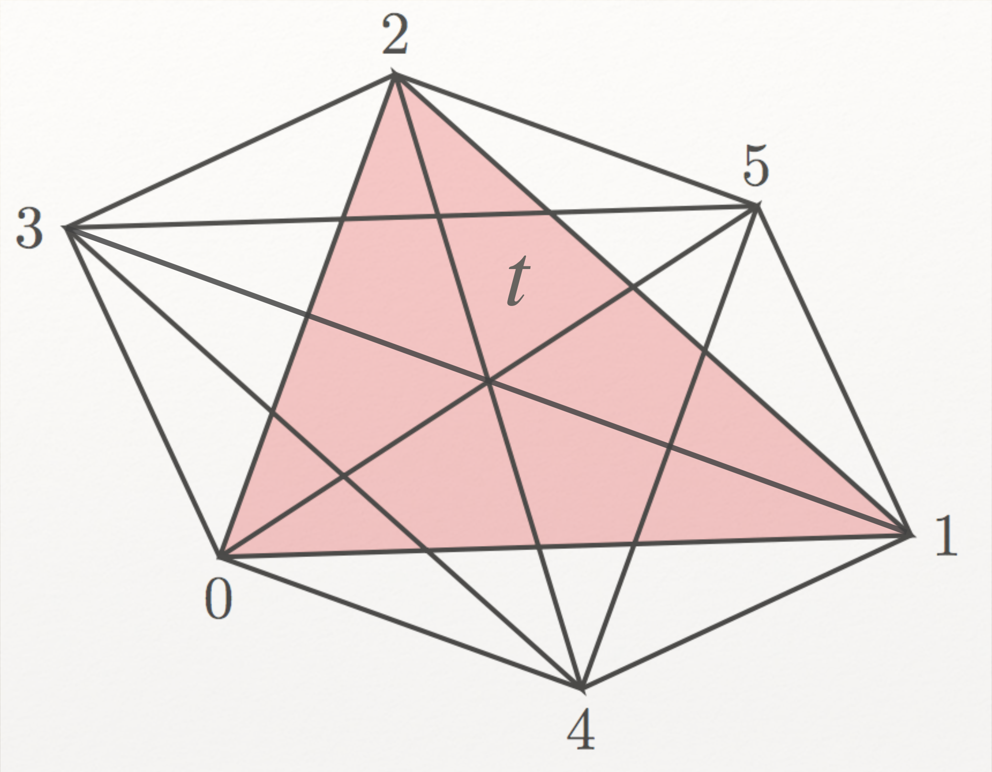

where

$$\epsilon_t = 2\pi - \sum_{\sigma \supset t} \theta_t^\sigma.$$

In Length Regge Calculus (LRC) we take

$$A_t = A_t(l) \quad \text{and} \quad \theta_t^\sigma = \theta_t^\sigma(l)$$

and varying S_{LRC} w.r.t. the bulk lengths l gives the eqs. of motion

$\displaystyle\sum_{t \supset e} \frac{\partial A_t}{\partial l_e} \epsilon_t(l) = 0,$ which limit, for finer & finer Δ, to the Einstein eqs.

In standard Regge Calculus we treat the lengths of edges as vars, while in Area Regge Calculus it's the areas of triangles

A 4-simplex has ten edges and ten faces. Locally the functions $A_t(l)$ can be inverted to give edge lengths $L^\sigma_e(a)$.

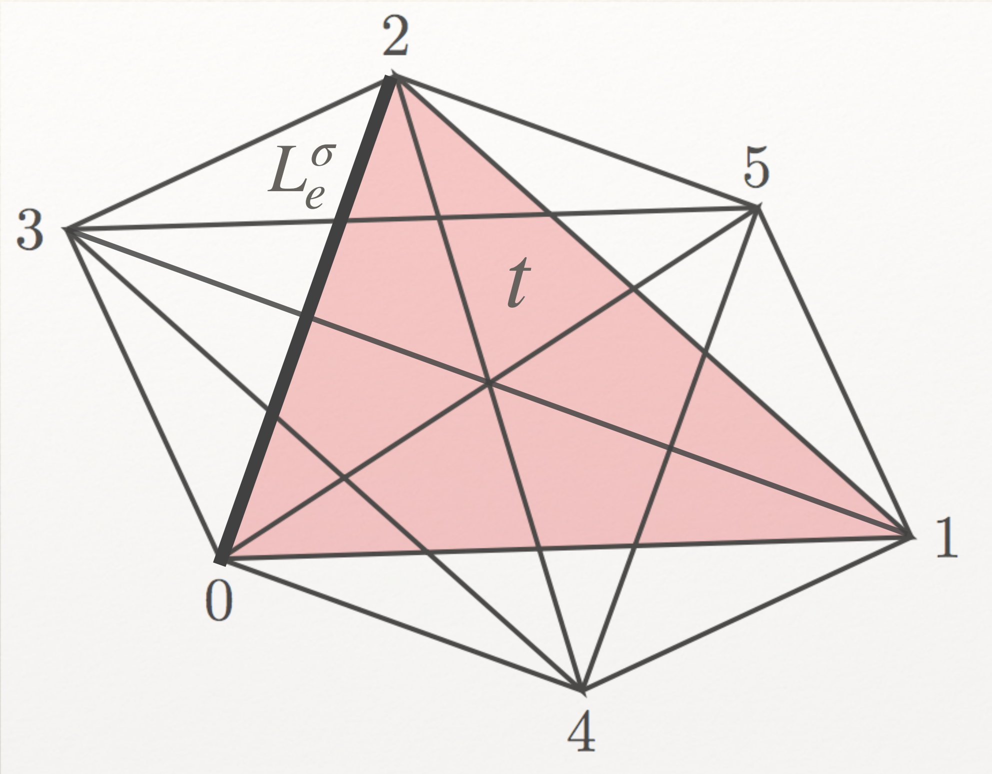

Considering areas a as variables we can define Area Regge Calculus (ARC) via the action

$$S_{\text{ARC}} = \sum_t a_t\, \epsilon_t(a)\ .$$

The dihedral and deficit angles are obtained using $\theta^\sigma_t(a) = \theta^\sigma_t(L^\sigma(a))$. Strikingly, variation of this action gives eqs. of motion

$$\delta S_{\text{ARC}} = \epsilon_t(a) + \cancel{\sum_t a_t \delta\epsilon_t} = \epsilon_t(a) = 0,$$ which impose flatness on Δ.

0 (due to the Schläfli identity)

Adding Constraints to the Theory

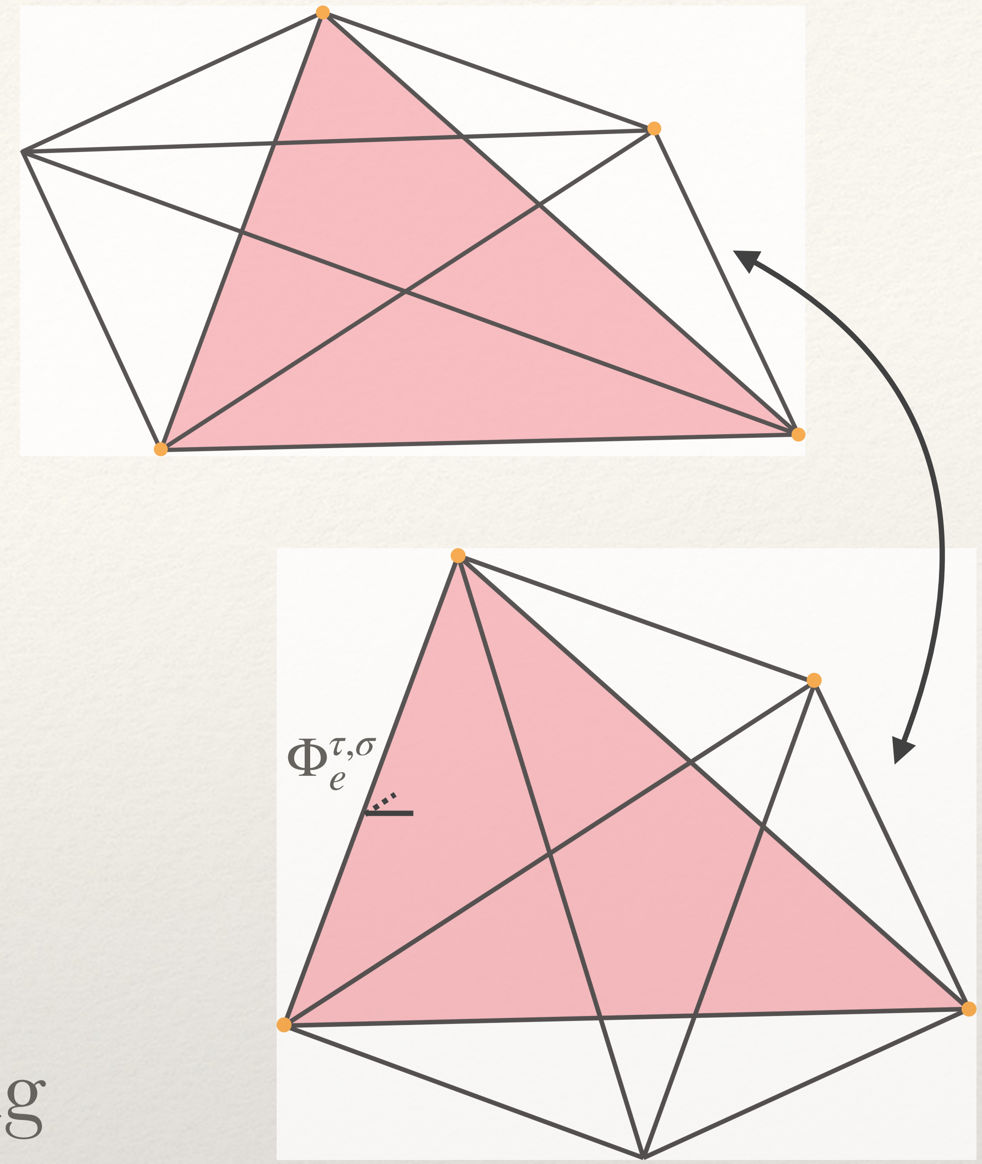

We can understand this difference in eqs. of motion between ARC and LRC as due to a differing # of degrees of freedom.

Gluing along the tetrahedron with orange vertices, 6 edge lengths are matched, but only 4 areas.

This mismatch can be resolved by introducing 3D dihedral angles:

$$\Phi_e^{\tau,\sigma}(a) = \Phi_e^{\tau}(L^{\sigma}(a)) \text{ is the dihedral angle around edge } e \text{ in tet } \tau.$$

Two neighboring simplices $\{\sigma, \sigma'\}$, glued along τ, will have the same lengths in τ if the constraints

$$\Phi_{e_i}^{\tau,\sigma}(a) - \Phi_{e_i}^{\tau,\sigma'}(a) = 0,\ i = 1,2 \text{ are imposed on non-opposite edges } e_i.$$

Adding Constraints to the Theory

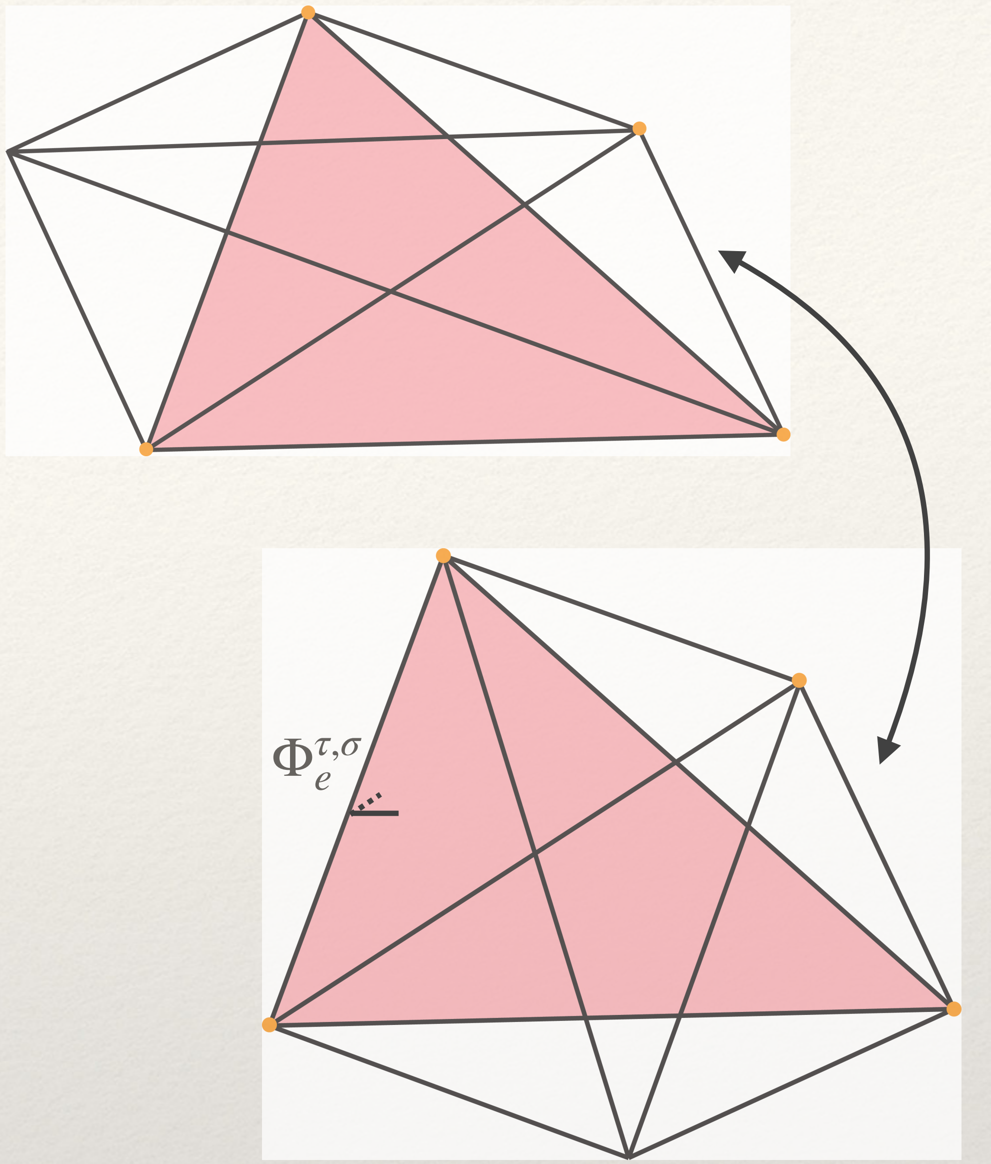

We can localize these constraints to a single 4-simplex by introducing two additional variables $\phi_{e_i}^\tau$ per τ to our theory and imposing

$$\phi_{e_i}^\tau - \Phi_{e_i}^{\tau,\sigma}(a) = 0, \quad i = 1,2.$$

The advantage of these localized constraints is that they preserve additive factorization of the Regge action and allow us to write the path integral in a product factorized form.

Dihedral angles at a pair of non-opposite edges (e_1, e_2) do not commute. Instead

$$\hbar\{\phi_{e_1}^\tau, \phi_{e_2}^\tau\} = \ell_P^2 \gamma \frac{\sin \alpha_v^{t,\tau}}{a_t} = \frac{\sin \alpha_v^{t,\tau}}{\left(j_t + \frac{1}{2}\right)}, \quad \text{with } \alpha_v^{t,\tau} \text{ the angle between } (e_1, e_2).$$

Adding Constraints to the Theory

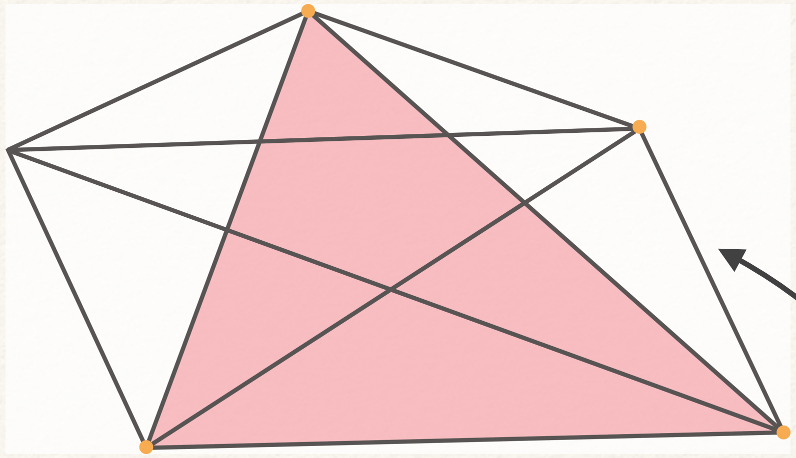

We can localize these constraints to a single 4-simplex by introducing two additional variables $\phi^{\tau}_{e_i}$ per τ to our theory and imposing

$$\phi^{\tau}_{e_i} - \Phi^{\tau,\sigma}_{e_i}(a) = 0, \quad i = 1,2.$$

2nd class constraints

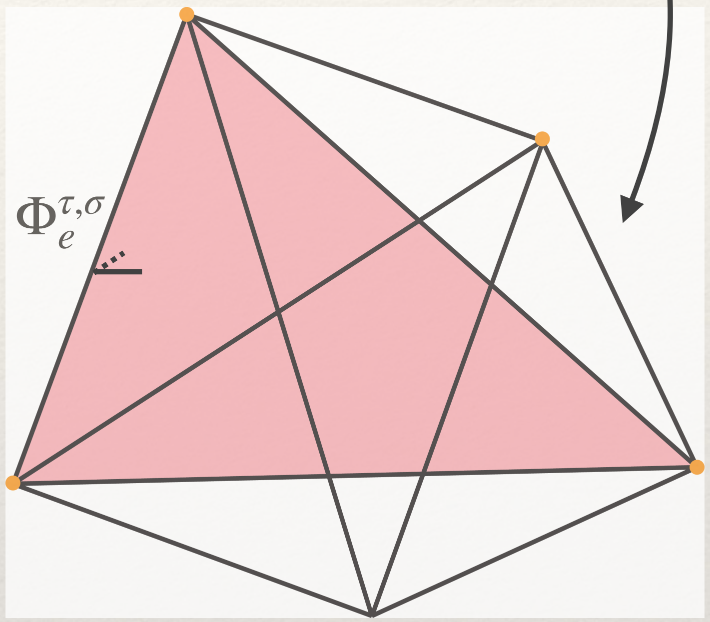

The advantage of these localized constraints is that they preserve additive factorization of the Regge action and allow us to write the path integral in a product factorized form.

Dihedral angles at a pair of non-opposite edges (e_1, e_2) do not commute. Instead

$$\hbar\{\phi^{\tau}_{e_1}, \phi^{\tau}_{e_2}\} = \ell_P^2 \gamma \frac{\sin \alpha_v^{t,\tau}}{a_t} = \frac{\sin \alpha_v^{t,\tau}}{\left(j_t + \frac{1}{2}\right)}, \quad \text{with } \alpha_v^{t,\tau} \text{ the angle between } (e_1, e_2).$$

The Area Regge action factorizes additively. Boundaries of the triangulation Δ are readily included.

From the definition of the deficit angle

$$\epsilon_t = 2\pi - \sum_{\sigma \supset t} \theta_t^\sigma,$$

we see that the area Regge action factorizes

$$S_{\text{ARC}} = \sum_t a_t \epsilon_t = \sum_t n_t \pi a_t - \sum_\sigma \sum_{t \supset \sigma} a_t \theta_t^\sigma(a) \equiv \sum_t S_t^a(a) + \sum_\sigma S_\sigma^a(a).$$

The last equality defines the triangle and simplex actions

$$S_t^a = n_t \pi a_t \quad \text{and} \quad S_\sigma^a(a) = - \sum_{t \supset \sigma} a_t \theta_t^a(L^\sigma(a)).$$

Here the index $n_t \in \{1,2\}$ allows for triangulations with boundary: it is 1 for triangles on the boundary and 2 for triangles in the bulk.

Defining our model

In this context we can define the spin foam

$$\mathcal{Z} = \sum_{\{j_t\}} \mu(j) \prod_t \mathcal{A}_t(j) \prod_\sigma \mathcal{A}_\sigma(j) \prod_{\tau \in \mathrm{blk}} G_\tau^{\sigma,\sigma'}(j),$$

with

$$\mathcal{A}_t = e^{\mathrm{i}\gamma n_t \pi (j_t + \frac{1}{2})} \qquad \text{and} \qquad \mathcal{A}_\sigma = e^{-\mathrm{i}\gamma \sum_{t \supset \sigma} (j_t + \frac{1}{2}) \theta_t^\sigma(j)}.$$

In practice, for our numerics we take $\mu(j) = 1$ for spins satisfying the constraints, but this deserves future study. (We could use a cosine too, a quite mild complication of our numerics; we focused on flatness.)

The factors $G_\tau^{\sigma,\sigma'}$ implement the constraints: imposing these sharply, with $G_\tau^{\sigma,\sigma'} = 1$ if satisfied and 0 else, leads to diophantine eqs. for the constraints that will only be satisfied for rare and special labels $\{j_t\}$;

the key fact that $\rightsquigarrow$ weak imposition of the constraints

We are forced to navigate between Scylla—reducing too much the density of states—and Charybdis—imposing dynamics that does not match GR

We implement the constraints with

Coherent state peaked on Φ's

$$G^{\sigma,\sigma'}_{\tau}(j) = \langle \mathscr{K}_{\tau}(\,\cdot\,; \Phi^{\tau,\sigma}_{e_i}(j)) \,|\, \mathscr{K}_{\tau}(\,\cdot\,; \Phi^{\tau,\sigma'}_{e_i}(j))\rangle.$$

Before proceeding to numerics, it's useful to note that, like other spin foams, this model can be derived from a constrained topological theory for GR—in this case a higher gauge theory

In this sense, this model is a fundamental spin foam.

Our calling these 'effective spin foams' is intended both to indicate the fact that with different G a variety of spin foams could be studied along these lines and to indicate these models' numerical efficiency.

The derivation from the BFCG higher gauge theory, shows that the amplitude factors

$$\mathscr{A}_t = e^{\mathrm{i}\gamma n_t \pi (j_t + \frac{1}{2})} \qquad \text{and} \qquad \mathscr{A}_\sigma = e^{-\mathrm{i}\gamma \sum_{t \supset \sigma} (j_t + \frac{1}{2}) \theta_t^\sigma(j)},$$

can be thought of as higher gauge recoupling coefficients; contrast the more familiar Wigner 3nj-symbols. This also exposes close connections with the Korepenov-Baratin-Freidel (KBF) model.

c.f Asante, Dittrich, Girelli, Riello, Tsimiklis; Korepenov; Baratin, Freidel; Mikovic, Oliveira, Vojinovic [1908.05970, 0211165, 0611042, 1508.05635]

Inputs and Approximations for the Numerics

The spin foam

$$\mathcal{Z} = \sum_{\{j_t\}} \mu(j) \prod_t \mathcal{A}_t(j) \prod_\sigma \mathcal{A}_\sigma(j) \prod_{\tau \in \mathrm{blk}} G_\tau^{\sigma,\sigma'}(j),$$

with $\mu(j) = 1$,

$$\mathcal{A}_t = e^{\mathrm{i}\gamma n_t \pi (j_t + \frac{1}{2})} \qquad \text{and} \qquad \mathcal{A}_\sigma = e^{-\mathrm{i}\gamma \sum_{t \supset \sigma} (j_t + \frac{1}{2}) \theta_t^\sigma(j)}.$$

To keep the numerics tractable we will:

- consider symmetry reduced triangulations
- approximate the coherent inner products by real gaussians with widths determined by the $\hbar\{\phi_{e_1}^\tau, \phi_{e_2}^\tau\} = \sin \alpha_v^{t,\tau} \left(j_t + \frac{1}{2}\right)^{-1}$ commutation relations
- We will also consider scaling with both j and γ.

Symmetry reduced numerical triangulation 1:
Δ contains three 4-simplices and one bulk triangle

There are three 4-simplices:

(12345), (12356), and (13456).

These share triangle (135).

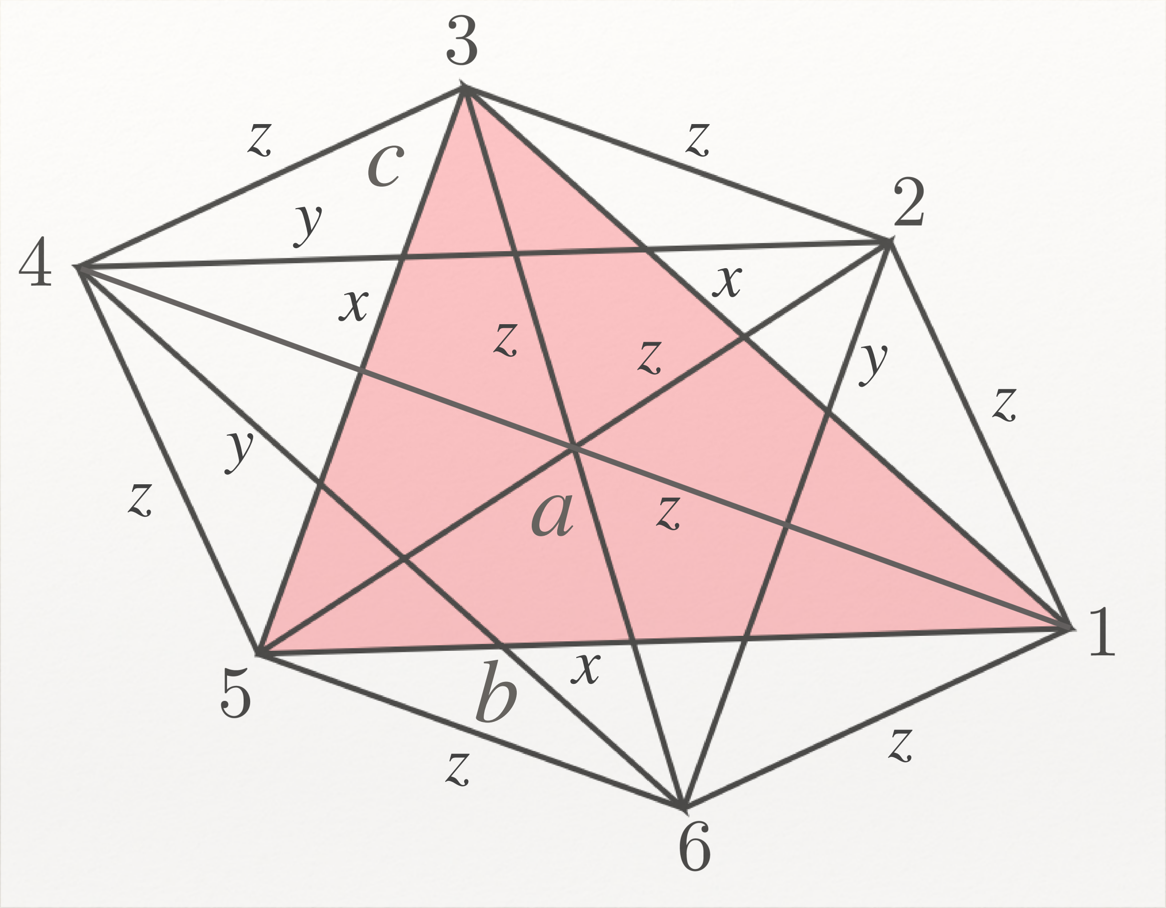

There are three independent lengths

$x = l_{ij}$ with $i, j = 1,3,5$

$y = l_{mn}$ with $m, n = 2,4,6$

$z = l_{im}$, all bndry z have dihedral ϕ_z.

Three independent areas: 2 bndry: $b = A(x, z, z)$, and $c = A(y, z, z)$,

and 1 blk: $a = A(x, x, x)$, which we sum over to get $\longrightarrow$ $\epsilon_a(b, c, \phi_z)$

Same Δ independently studied in $SU(2)$ BF theory in recent paper by Donà, Gozzini, Sarno [2004.12911]

Numerical results on triangulation 1: Gluing two such Δ along their bndrys we get a triangulation of the boundary-less S^4

Let a be the bulk area of the first copy and a' that of the second. Fix a', b, c.

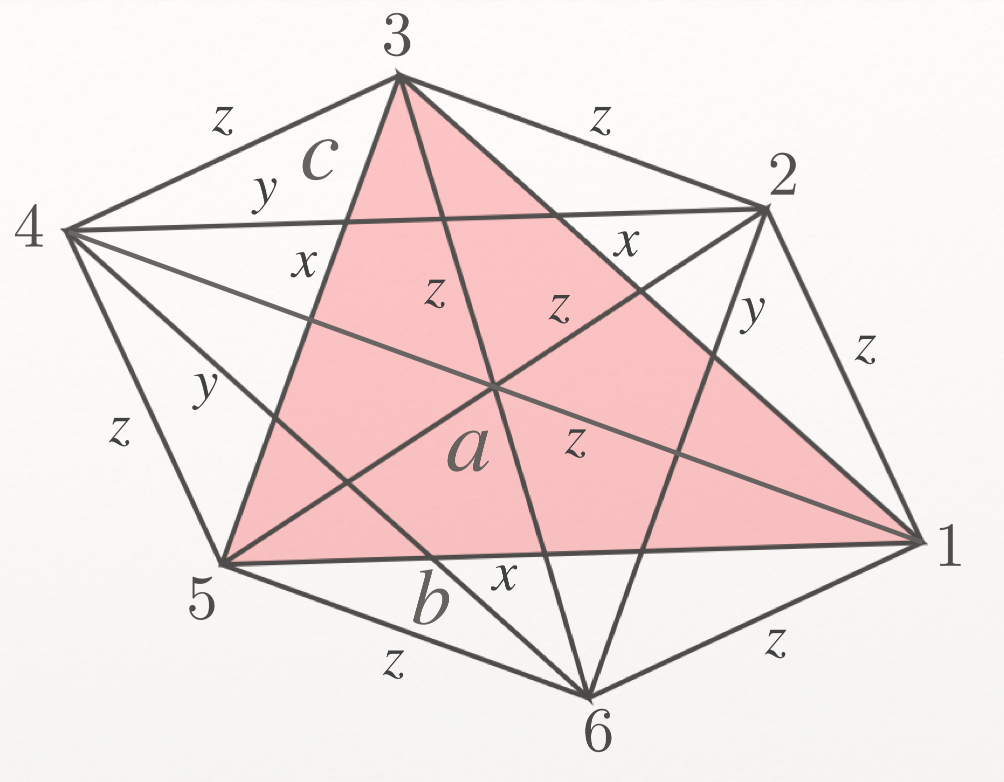

Compute:

$$\langle \epsilon_a \rangle (a', b, c) = \frac{1}{\mathcal{Z}} \sum_{j_a} \epsilon_a G(a, a') \prod_t \mathcal{A}_t \prod_\sigma \mathcal{A}_\sigma$$

with

$$G = \exp\left\{ -\frac{9}{2\sigma(\Phi)^2} \left[\Phi_z(a, b, c) - \Phi_z(a', b, c)\right]^2 \right\}$$

and

$$\sigma^2(\Phi) = \frac{1}{2} \frac{\sin\alpha(a, b, c)}{\left(j_b + \frac{1}{2}\right)} + \frac{1}{2} \frac{\sin\alpha(a', b, c)}{\left(j_b + \frac{1}{2}\right)}, \quad \sin\alpha(a, b, c) = \frac{2b}{z^2(a, b, c)}.$$

Numerical results on triangulation 1: The $\mathscr{A}$'s oscillate, the G are gaussian—need gradual oscillations to not kill G constraints

Compute:

$\langle \epsilon_a \rangle (a', b, c) =$

$$\frac{1}{\mathcal{Z}} \sum_{j_a} \epsilon_a G \prod_t \mathscr{A}_t \prod_\sigma \mathscr{A}_\sigma$$

$(j+\frac{1}{2}, j_{a'}+\frac{1}{2}, \epsilon_{a'})$	$\gamma = 0.01$	$\gamma = 0.1$	$\gamma = 0.5$
(30, 38.5, 0.52)	0.78 – 0.03i	0.68 – 0.26i	0.17 – 0.32i
(100, 128, 0.54)	0.62 – 0.062i	0.55 – 0.19i	0.17 – 0.27i
(300, 384, 0.54)	0.57 – 0.02i	0.51 – 0.17i	0.16 – 0.25i
(1000, 1280, 0.54)	0.55 – 0.01i	0.50 – 0.16i	0.16 – 0.24i

Boundary induces classical (LRC) value of $\epsilon_a \approx 0.5$

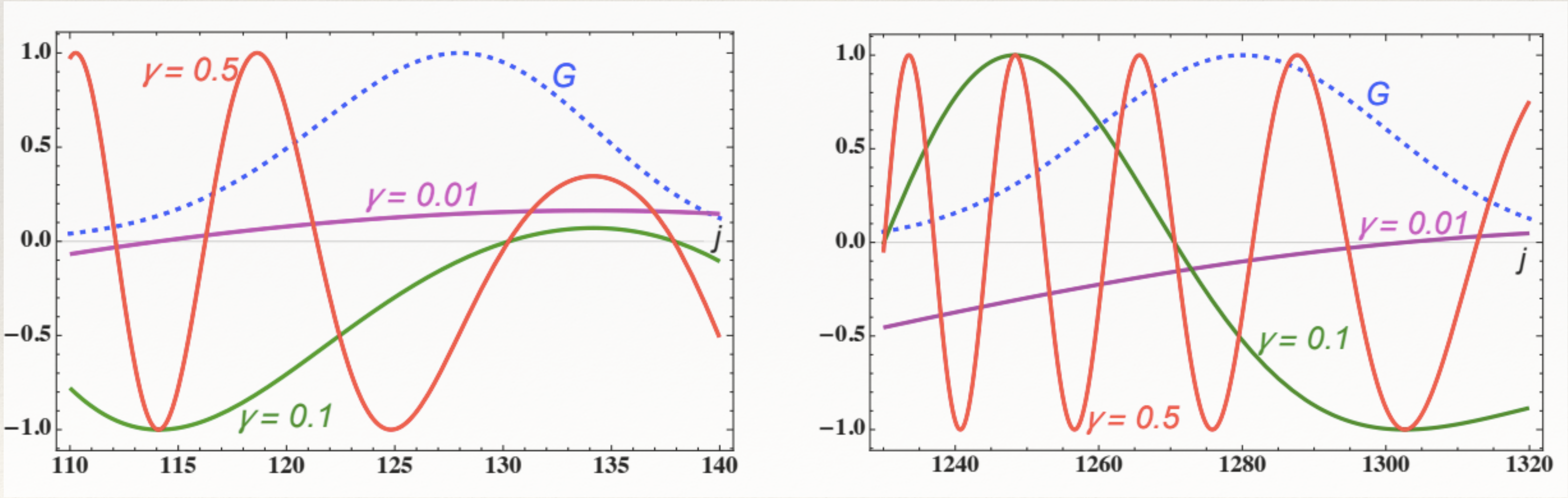

$j = 99.5$ $\qquad$ $j = 999.5$

It may come as a surprise that a good semiclassical geometry is achieved for large j *and* small γ—a scaling argument illustrates why

An important input for us is that $\hbar\{\phi^\tau_{e_1}, \phi^\tau_{e_2}\} = \sin\alpha^{t,\tau}_v \left(j_t + \frac{1}{2}\right)^{-1}$ determines the width of G:

$$\sigma(\Phi) \sim 1/\sqrt{j}.$$

Consider Δ to have nearly equal bndry areas $a \sim \gamma \ell_P^2 j$, hence $a_{\rm blk} \sim a$. Then scaling wise, we have

$$\sigma(j_{\rm blk}) \sim \left[\frac{\partial \Phi(j_{\rm blk})}{\partial j_{\rm blk}}\right]^{-1} \times \sigma(\Phi) \sim j \times \frac{1}{\sqrt{j}} = \sqrt{j}\ ,$$

$$\sigma(\epsilon) \sim \left[\frac{\partial \epsilon(j_{\rm blk})}{\partial j_{\rm blk}}\right] \times \sigma(j_{\rm blk}) \sim \frac{1}{j} \times \sqrt{j} = \frac{1}{\sqrt{j}}.$$

Can peak on $\epsilon \neq 0$, $\rightsquigarrow$ large j, summation range grows & need to require

$$\sigma\left(\frac{S_{\rm ARC}}{\ell_P^2}\right) = \frac{1}{\ell_P^2}\frac{\partial S_{\rm ARC}}{\partial j_{\rm blk}} \times \sigma(j_{\rm blk}) \sim \gamma\epsilon\sqrt{j} \lesssim \mathcal{O}(1).$$

C.f. Han [1304.5628]

Symmetry reduced numerical triangulation 2:

Δ consists of 6 simplices around one edge

We apply a certain symmetry reduction, so that there are only 3 bndry and 3 bulk areas (4 bndry lengths and 1 bulk length).

There are 3 simplices of type 1 and three simplices of type 2. In each type, all simplices have the same geometry.

The path integral involves 1 bulk variable in LRC and 3 area variables in (constrained) ARC. However, making use of the fall off of the G functions, we can significantly reduce the summation range and gain time savings in the numerics.

Symmetry reduced numerical triangulation 2:

Δ consists of 6 simplices around one edge

For completeness, here is the definition of this Δ:

vertices:	m,n=0,1; i,j=2,3,4	k=5,5′
simplices:	(0,1,2,3,5)	(01,2,3,5′)
	(0,1,2,4,5)	(0,1,2,4,5′)
	(0,1,3,4,5)	(0,1,3,4,5′)
lengths:	$l_{01} = t$ blk	$l_{01} = t$ blk
	$l_{mi} = l_{ik} \equiv x$	$l_{mi} = l_{ik} \equiv x$
	$l_{ij} \equiv y$	$l_{ij} \equiv y$
	$l_{m5} \equiv z$	$l_{m5'} \equiv z'$
areas:	$A(x, x, y)$	$A(x, x, y)$
	$A(x, x, t)$ blk	$A(x, x, t)$ blk
	$A(x, x, z)$	$A(x, x, z')$
	$A(z, z, t)$ blk	$A(z', z', t)$ blk

A set of generalized triangle inequalities restricts the bulk areas of this Δ to particular ranges

Within the triangle allowed region, only a small part of the parameter space has non-negligible values of G.

In this numerical example, it is the portion at the lower left of the figure.

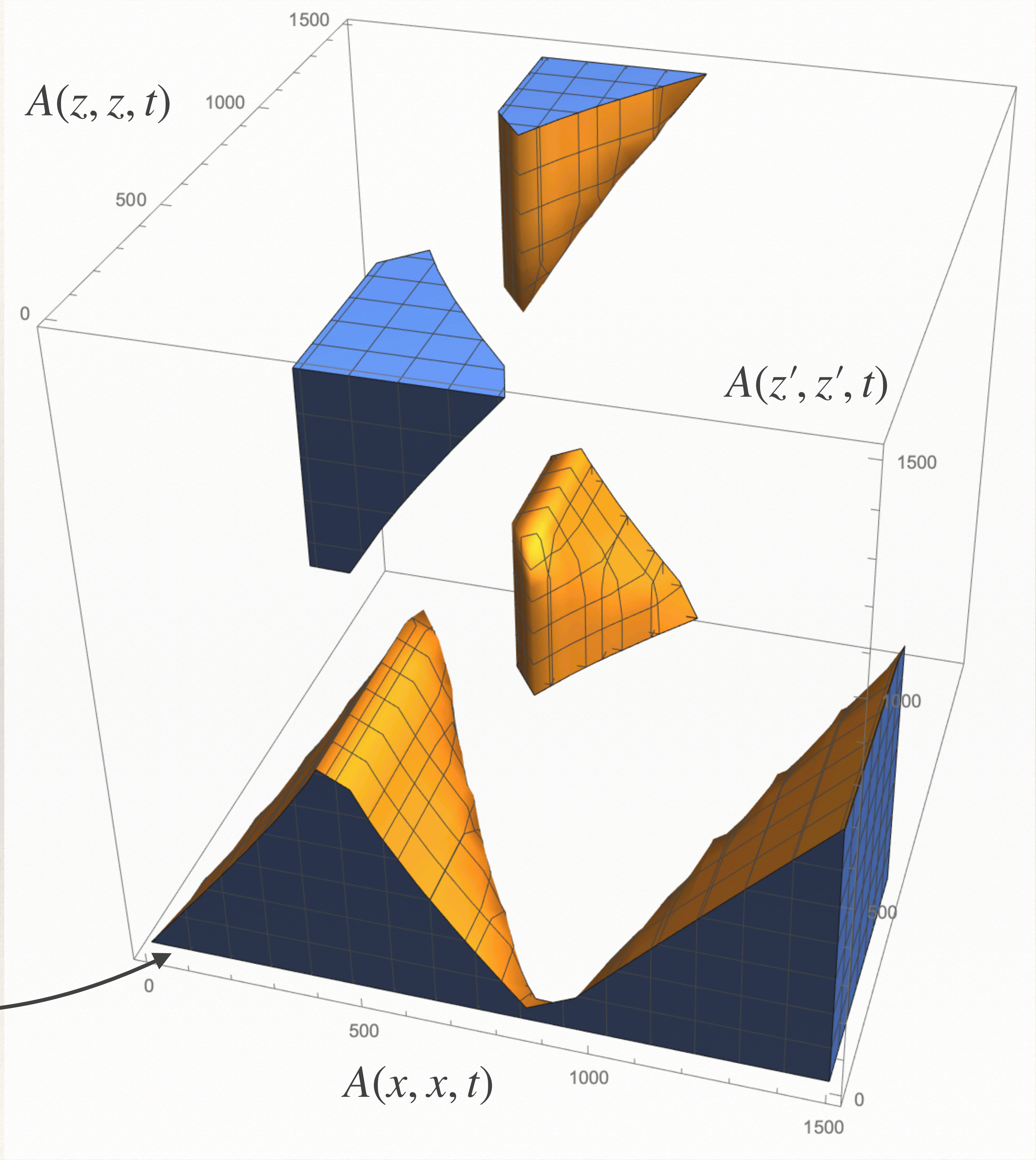

Indeed, the region of non-negligible G is even smaller

Within the blue region the (generalized) triangle inequalities are satisfied.

Within the gold strip the value of G is greater than 10^{-10}.

These dual conditions greatly restrict the range of summation and increase the speed of the numerics.

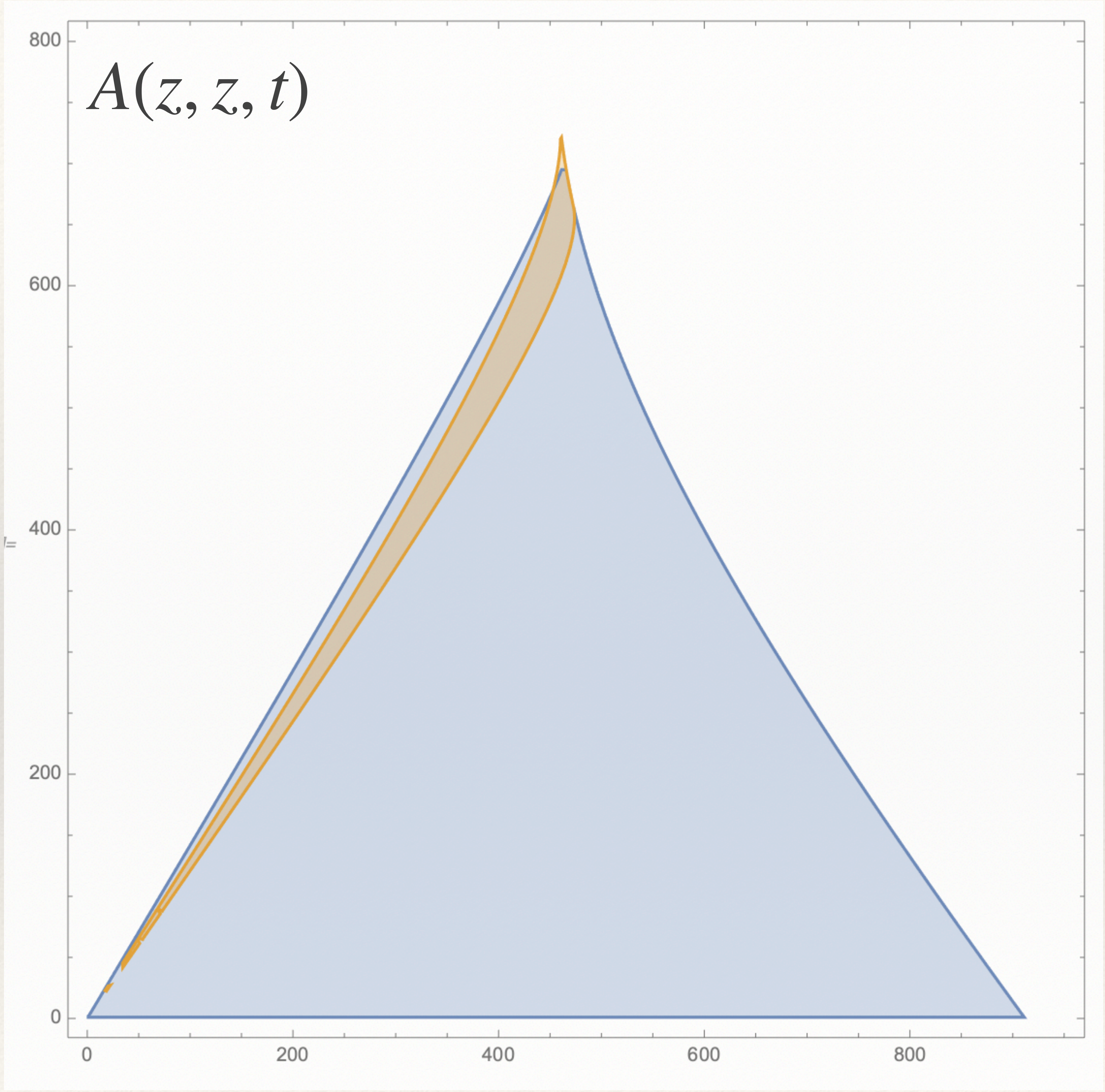

$A(x, x, t)$

On our methodology: amongst the three bulk areas, there is a combination of variations consistent with the constraints

There are 3 bndry and 3 bulk areas (4 bndry and 1 bulk length).

In effect, the G limit us to the swath of parameter space around the bulk length variation by keeping us near to shape matched configs.

So far through expectation values, we investigate whether, for large j, there is a value of γ that gives us expectation values consistent with LRC.

If we were doing a saddle point analysis, approximating sums by integrals, these would be saddles of the ARC action but only along the constraint directions. Perhaps it is useful to call these semi-saddles. By construction these semi-saddles agree with the LRC saddles as well as the (weak) constraints allow.

An example of a triangulation of this sort, call it Δ_1

Fix the three bndry areas to have values:

$$A(x,x,y)=456, \qquad A(x,x,z)=456, \qquad A(x,x,z')=443$$

The nearest LRC solution has bulk areas given by

$$A(x,x,t)=463.07, \quad A(z,z,t)=673.47, \quad A(z',z',t)=607.08$$

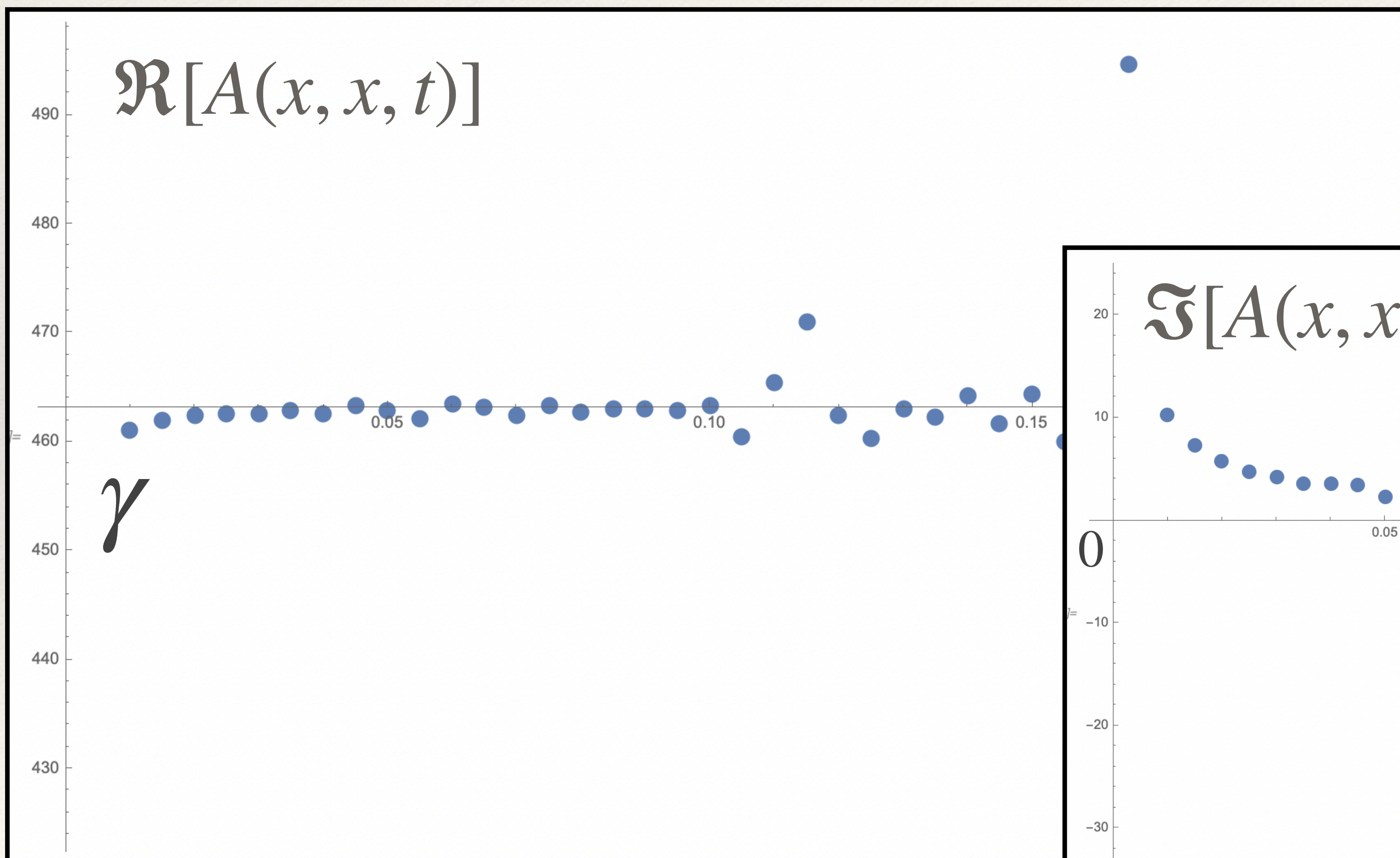

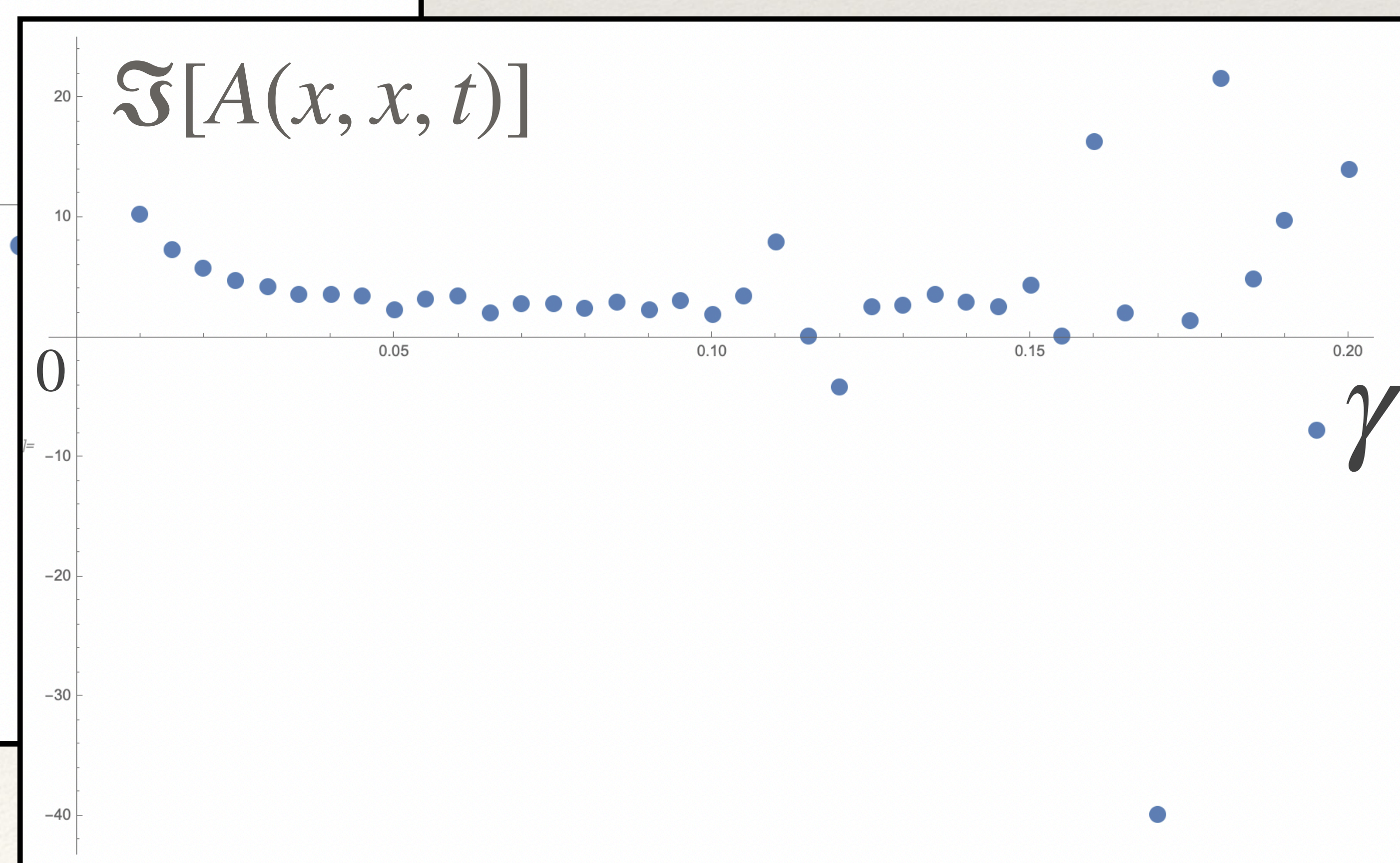

An example of a triangulation of this sort, call it Δ_1

Fix the three bndry areas to have values:

$A(x,x,y)=456, \qquad A(x,x,z)=456, \qquad A(x,x,z')=443$

The nearest LRC solution has bulk areas given by

$A(x,x,t)=463.07, \quad A(z,z,t)=673.47, \quad A(z',z',t)=607.08$

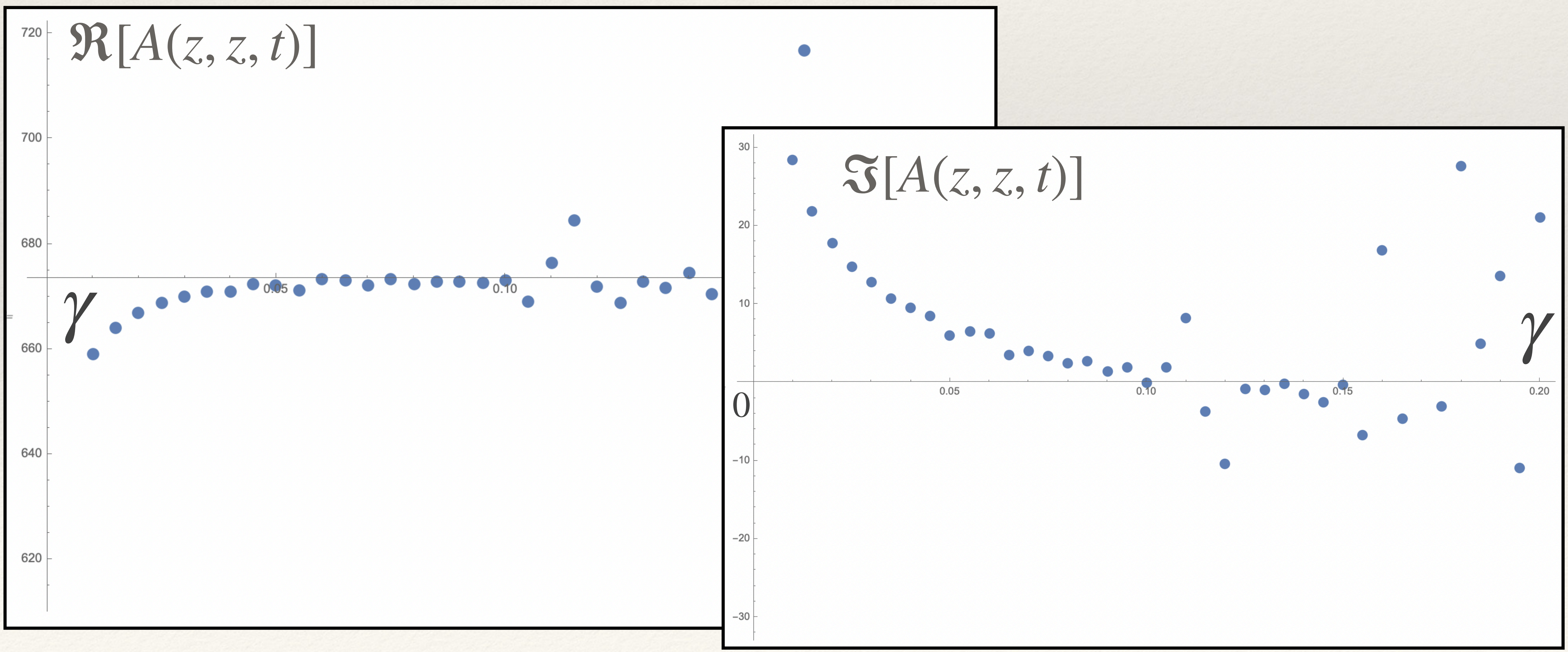

An example of a triangulation of this sort, call it Δ_1

Fix the three bndry areas to have values:

$$A(x,x,y)=456, \qquad A(x,x,z)=456, \qquad A(x,x,z')=443$$

The nearest LRC solution has bulk areas given by

$$A(x,x,t)=463.07, \quad A(z,z,t)=673.47, \quad A(z',z',t)=607.08$$

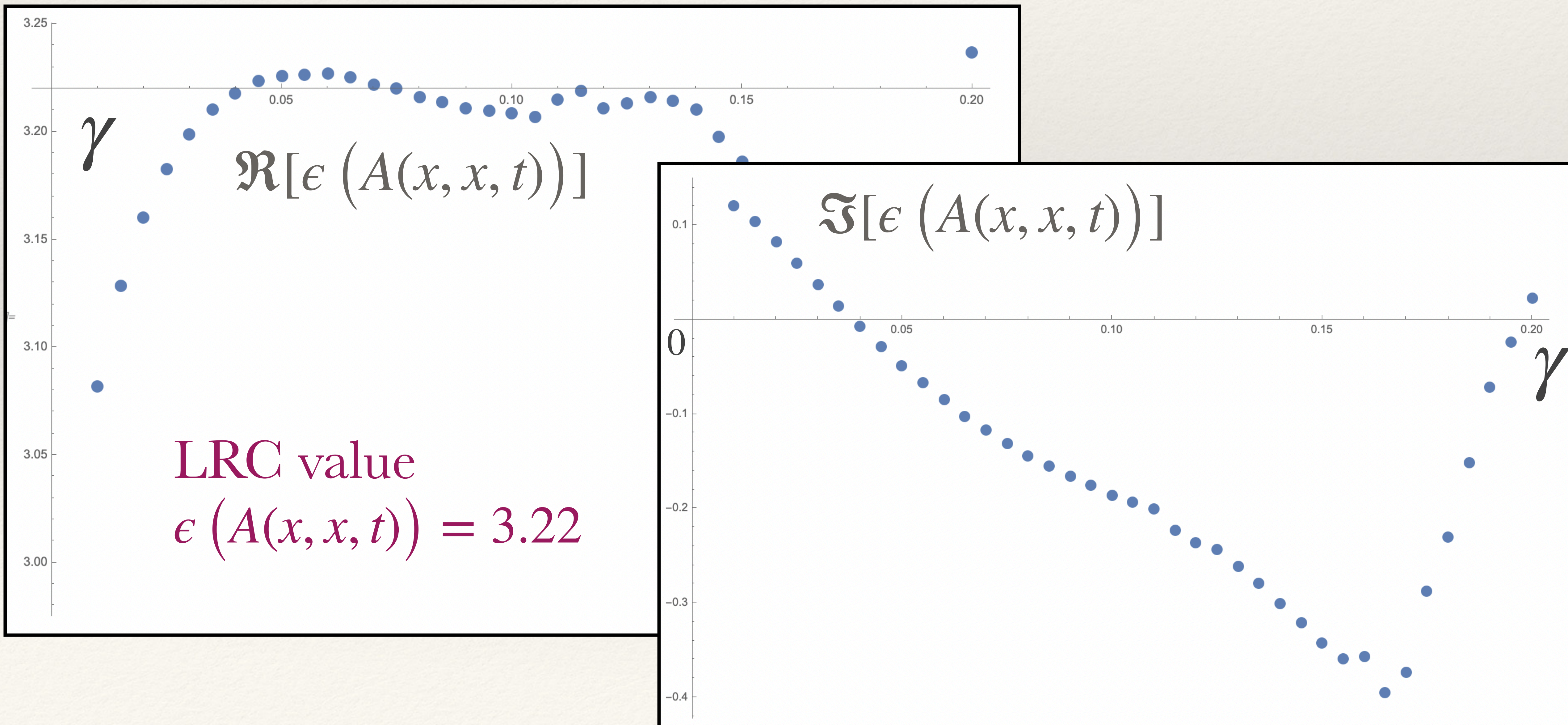

A 2nd example of a triangulation of this sort, call it Δ_2

Fix the three bndry areas to have values:

$$A(x,x,y)=912, \qquad A(x,x,z)=912, \qquad A(x,x,z')=886$$

The nearest LRC solution has bulk areas given by

$$A(x,x,t)=926.13, \quad A(z,z,t)=1346.94, \quad A(z',z',t)=1214.15$$

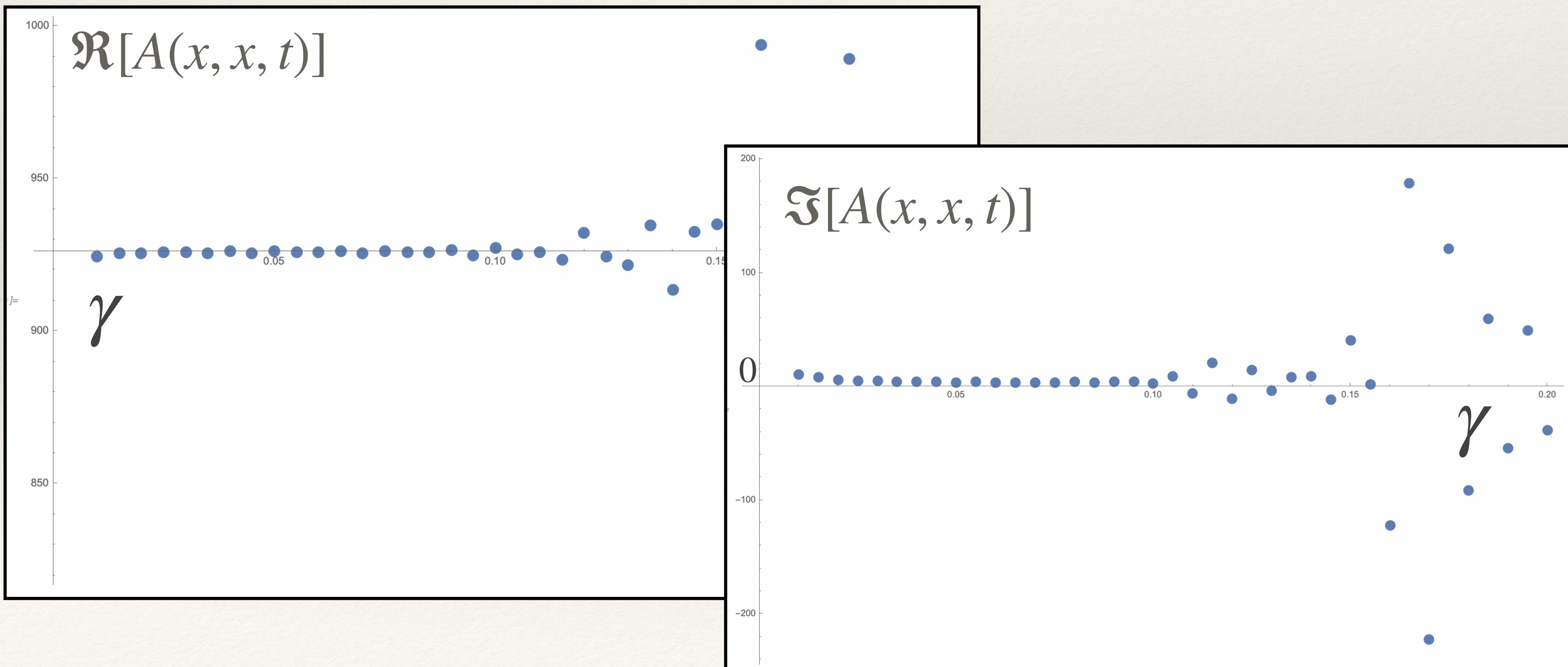

A 2nd example of a triangulation of this sort, call it Δ_2

Fix the three bndry areas to have values:

$$A(x,x,y)=912, \qquad A(x,x,z)=912, \qquad A(x,x,z')=886$$

The nearest LRC solution has bulk areas given by

$$A(x,x,t)=926.13, \quad A(z,z,t)=1346.94, \quad A(z',z',t)=1214.15$$

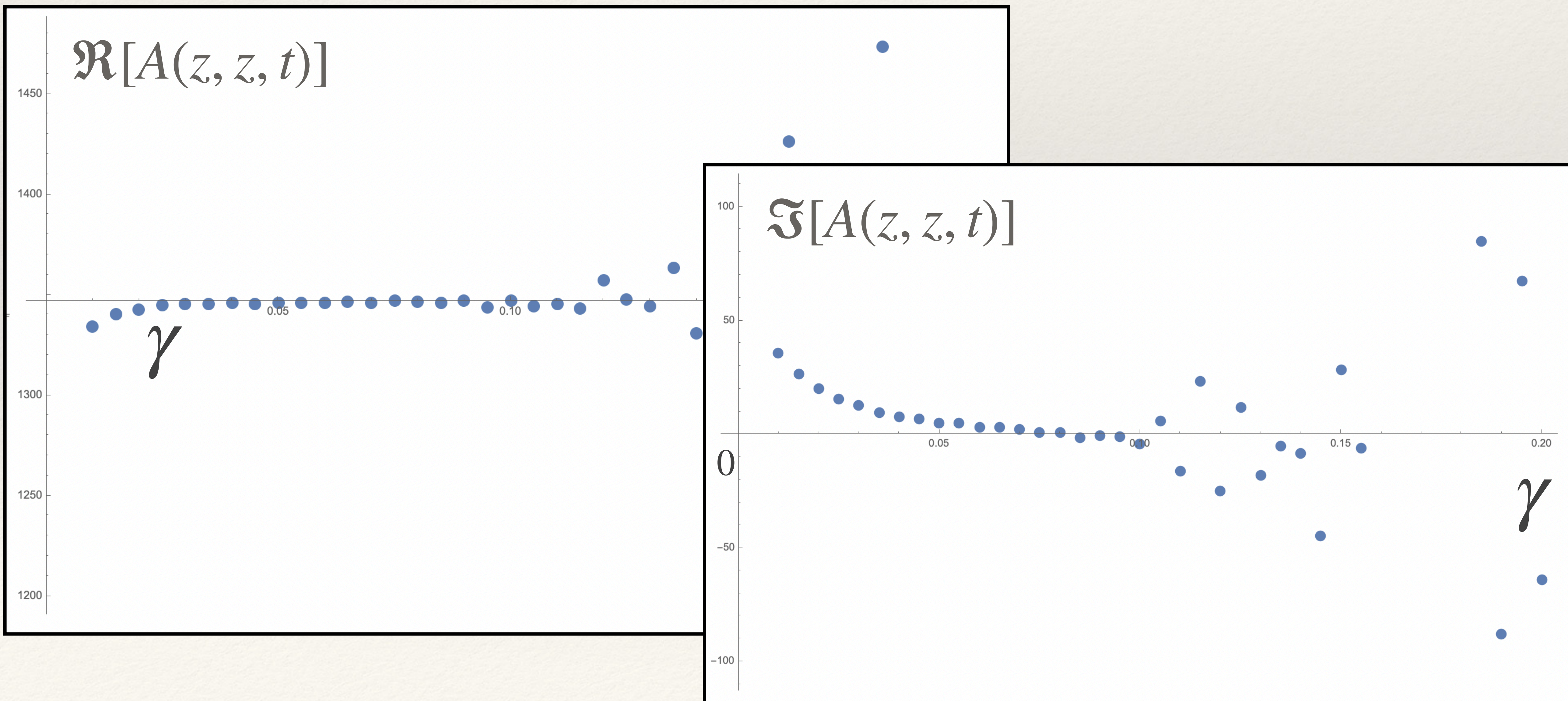

A 2nd example of a triangulation of this sort, call it Δ_2

Fix the three bndry areas to have values:

$$A(x,x,y)=912, \quad A(x,x,z)=912, \quad A(x,x,z')=886$$

The nearest LRC solution has bulk areas given by

$$A(x,x,t)=926.13, \quad A(z,z,t)=1346.94, \quad A(z',z',t)=1214.15$$

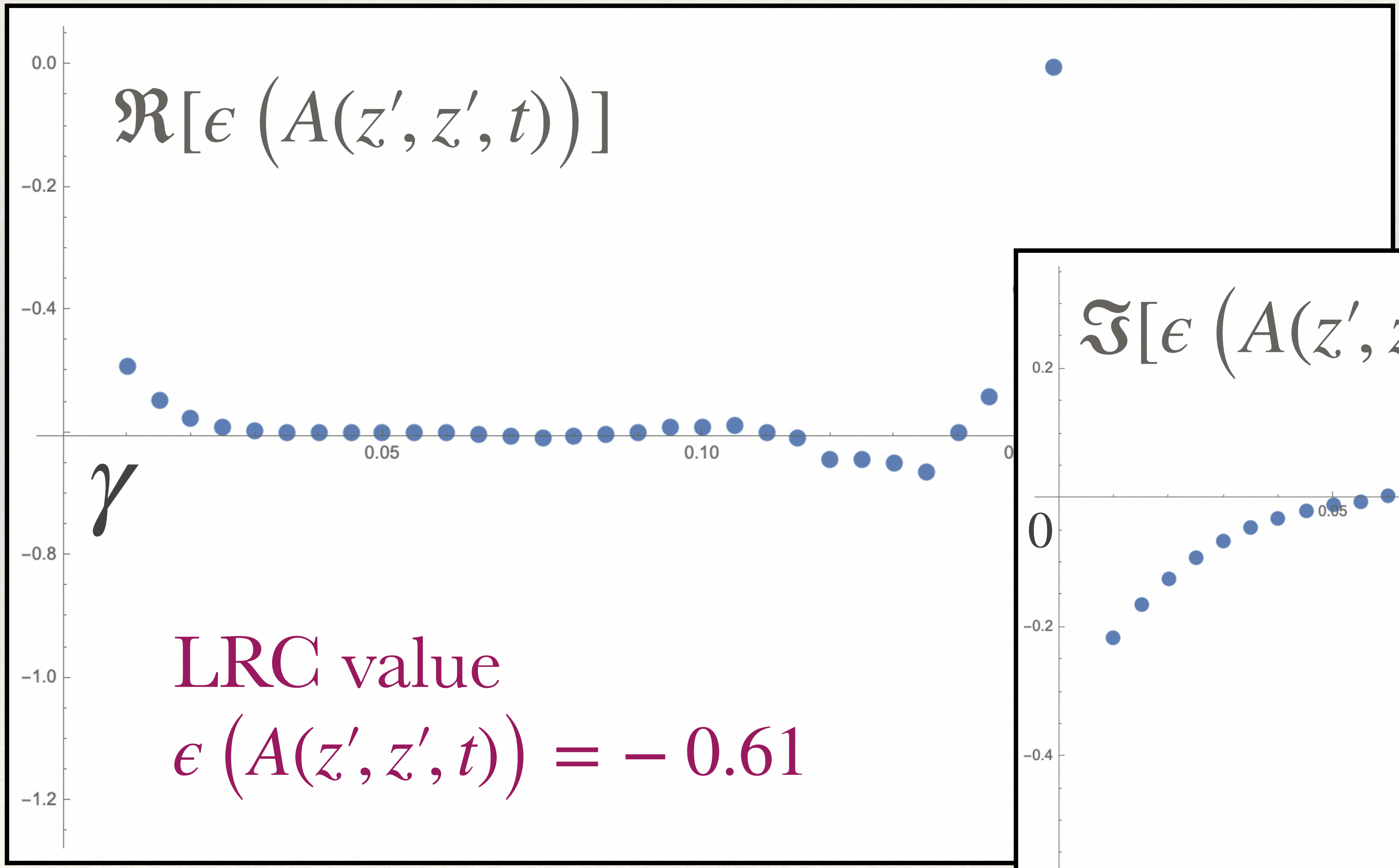

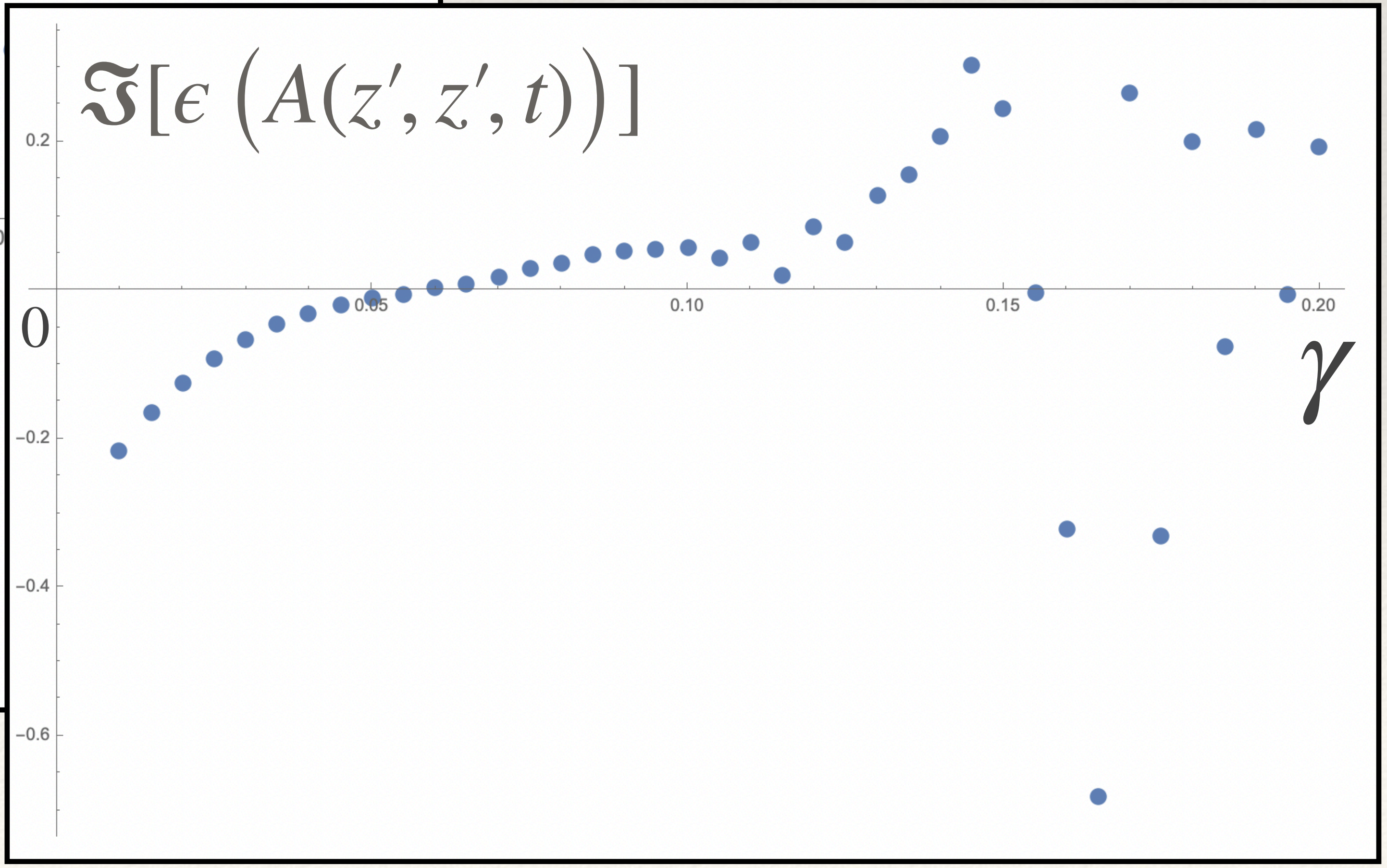

We also studied a 3rd example with bndry values $\Delta_3 = 3 \cdot \Delta_1$.
Here are comparisons of all 3 exs. rescaled by LRC values:

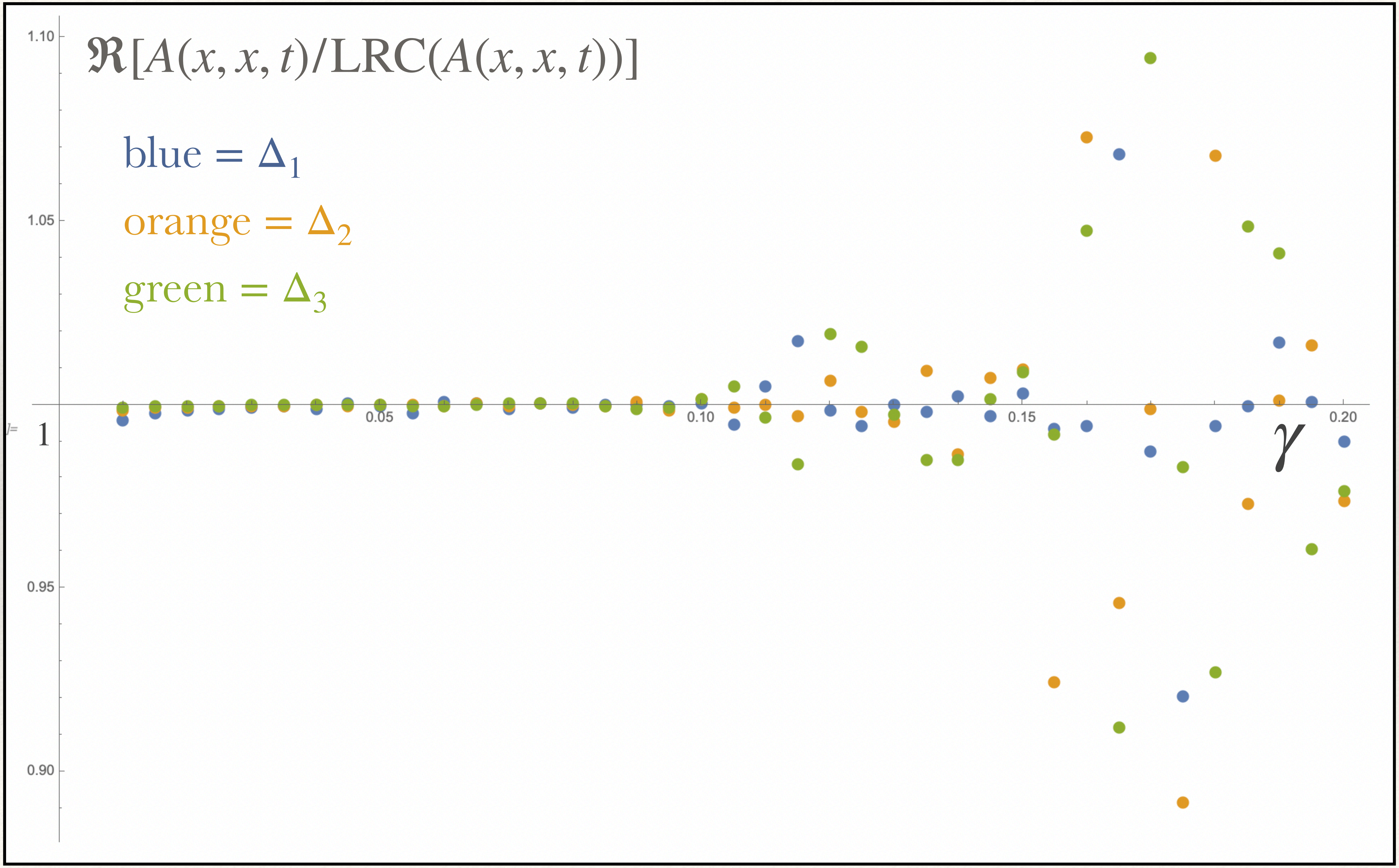

We also studied a 3rd example with bndry values $\Delta_3 = 3 \cdot \Delta_1$.
Here is a comparison of the deficit around $A(x,x,t)$:

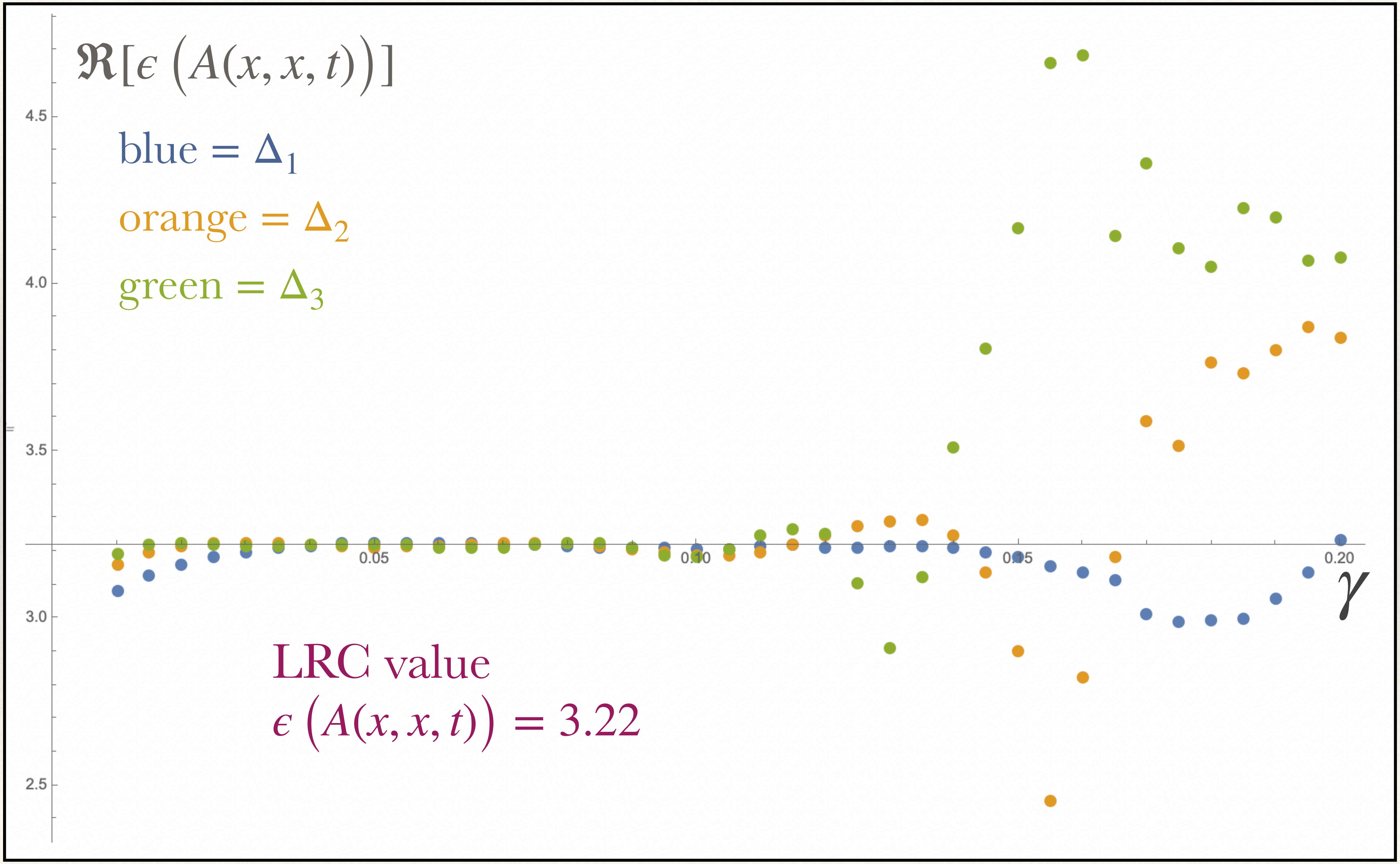

All computations were performed on laptops using Mathematica. In each run we computed 6 expectation values for 40 different values of γ, for a total of 240 spin foam sums

Classical area values	Maximum bulk spins	Time
J1 = 0.5* 463.07, J2 = 0.5* 673.47, J3 = 0.5* 607.08	J1 = 245, J2 = 395, J3 = 350	~6 mins
J1 = 463.07, J2 = 673.47, J3 = 607.08	J1 = 475, J2 = 732, J3 = 661	~25 mins
J1 = 2*463.07, J2 = 2*673.47, J3 = 2* 607.08	J1 = 950, J2 = 1452, J3 = 1316	~5 hrs
J1 = 3*463.07, J2 = 3*673.47, J3 = 3* 607.08	J1 = 1420, J2 = 2162, J3 = 2121	***~20+ hrs***

A table of the time to make one such run. This depends on the values of the boundary spins, which determine the range of bulk spins that one must sum over.

This computational framework is remarkably fast and allows numerical exploration of many interesting questions.

Expectations/Conjectures from steepest descent and Picard-Lefschetz Theory

We have ***not*** yet explored complex values for our parameters. Hence, what appears here should be viewed as conjectures only.

In both examples presented here, the 3 simplices with a bulk triangle and 6 simplices with an inner edge, we found complex expectation values for the deficit angles around bulk triangles.

We conjecture that these complex expectation values are from saddles that are slightly off in the complex plane. We believe we may have identified a regime in which a saddle moves close to the real axis. This may be one characterization of what is desirable about our conditions on γ & j.

Expectations/Conjectures from steepest descent and Picard-Lefschetz Theory

The picture that we have in mind is like that of Picard-Lefschetz theory, where an initial contour is deformed onto the steepest descent contour and the integral can be well approximated asymptotically by its value at the complex saddle.

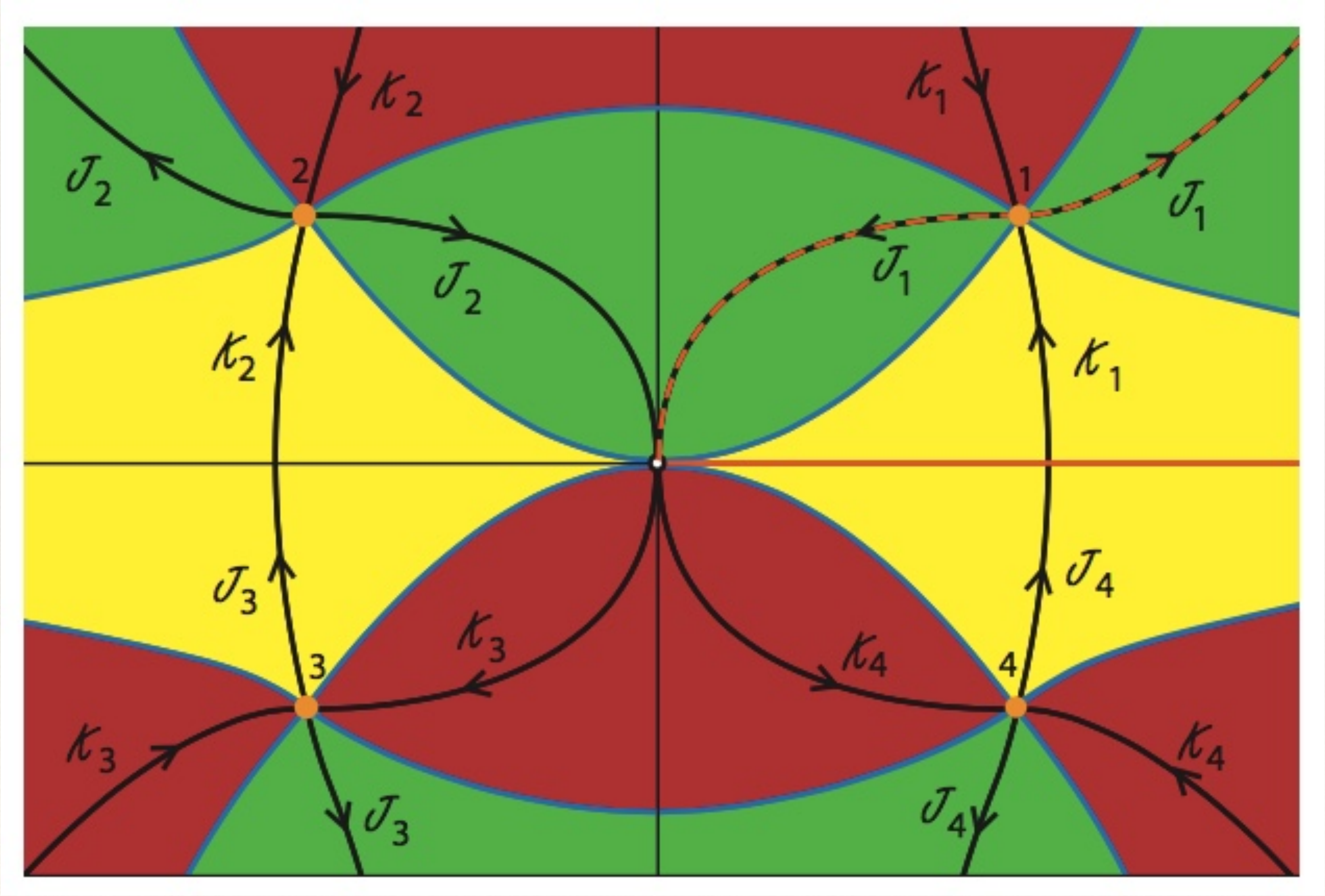

This model illustrates that spin foams can avoid the flatness problem in a range of spin j and Barbero-Immirzi parameter γ

E.g. at $\gamma = 0.1$, for Δ_3 we have

$$\epsilon(A(x,x,t)) = 3.19 - 0.20i, \quad \epsilon(A(z,z,t)) = -1.32 + 0.18i, \text{ and}$$

$$\epsilon(A(z',z',t)) = -0.59 + 0.07i$$

Compare the LRC values:

$\epsilon(A(x,x,t)) = 3.22$

$\epsilon(A(z,z,t)) = -1.36$

and

$\epsilon(A(z',z',t)) = -0.607$

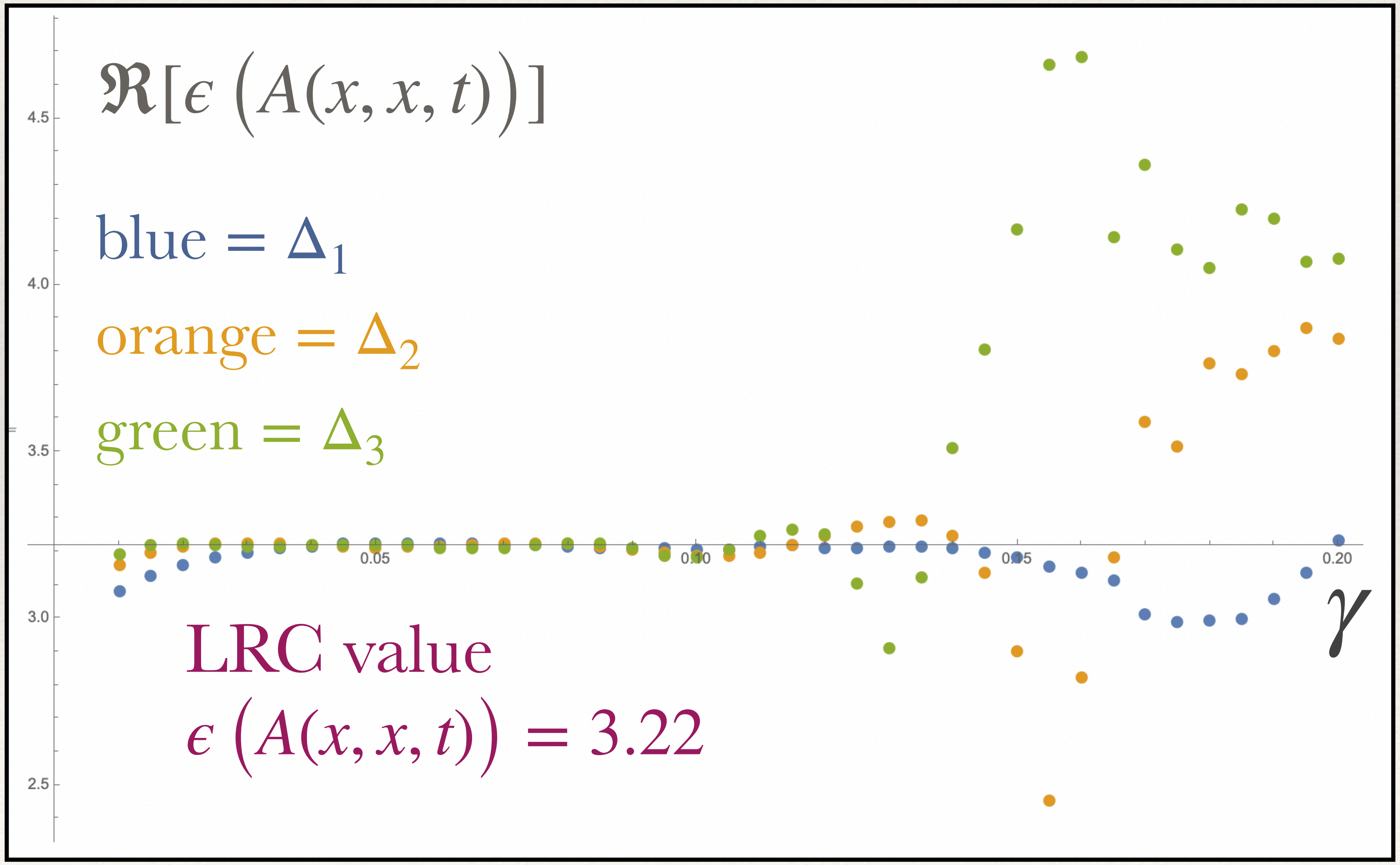

Conclusions

We have introduced a new spin foam model

$$\mathcal{Z} = \sum_{\{j_t\}} \mu(j) \prod_t \mathcal{A}_t(j) \prod_\sigma \mathcal{A}_\sigma(j) \prod_{\tau \in \mathrm{blk}} G_\tau^{\sigma,\sigma'}(j),$$

with $\mathcal{A}_t = e^{\mathrm{i}\gamma n_t \pi (j_t + \frac{1}{2})}$ and $\mathcal{A}_\sigma = e^{-\mathrm{i}\gamma \sum_{t \supset \sigma} (j_t + \frac{1}{2}) \theta_t^\sigma(j)}$.

The functions G implement the second class constraints coming from shape matching in a manner consistent with the LQG Hilbert space.

▲ Constrained theories with discrete geometric spectra can suffer from too low a density of states: diophantine conditions arising from the discreteness make strong imposition a stringent requirement

▲ Nonetheless weak imposition of the constraints can be consistent with the dynamics of General Relativity, as indicated by our numerics

▲ This model allows for rapid numerical simulation and the exploration of a landscape of interesting questions in spin foams

Thank you!